Turkish Journal of Earth Sciences (Turkish J. Earth Sci.), Vol. 20, 2011, pp. 57–98. Copyright ©TÜBİTAK
doi:10.3906/yer-0910-8 First published online 01 May 2010

TÜBİTAK

Geology and Correlation of the Mersin Mélanges, Southern Turkey

PATRICE MOIX[1], LAURENT BECCALETTO[2], OLIVIER MASSET[3], HEINZ W. KOZUR[4], PAULIAN DUMITRICĂ[5], DANIEL VACHARD[6], ROSSANA MARTINI[7] & GÉRARD M. STAMPFLI[1]

[1] Institute of Geology and Palaeontology, Université de Lausanne, 1015 Lausanne, Switzerland
(E-mail: patricemoix@gmail.com)

[2] BRGM – Service GEOlogie / Géologie des bassins sédimentaires, 3 Av. Cl. Guillemin – BP 36009, 45060 Orléans Cedex 2, France

[3] ETH Zürich-Geologisches Institut, Wolfgang-Pauli Strasse 15, 8093 Zürich, Switzerland

[4] Rézsü u. 83, 1029 Budapest, Hungary

[5] Dennigkofenweg 33, 3073 Gümligen, Switzerland

[6] UMR 8157 du CNRS 'Géosystèmes', Université de Lille 1, Bâtiment SN5, 59655 Villeneuve d'Ascq Cedex, France

[7] Department of Geology and Palaeontology, University of Geneva, 1205 Geneva, Switzerland

Received 11 October 2009; revised typescript receipt 01 February 2010; accepted 01 May 2010

Abstract: Our paper aims to give a thorough description of the infra-ophiolitic mélanges associated with the Mersin ophiolite. We propose new regional correlations of the Mersin mélanges with other mélange-like units or similar series, located both in southern Turkey and adjacent regions. The palaeotectonic implications of the correlations are also discussed. The main results may be summarized as follows: the infra-ophiolitic mélange is subdivided into two units, the Upper Cretaceous Sorgun ophiolitic mélange and the Ladinian–Carnian Hacialanı mélange. The Mersin mélanges, together with the Antalya and Mamonia domains, are represented by a series of exotic units now found south of the main Taurus range, and are characteristic of the South-Taurides Exotic Units. These mélanges clearly show the mixed origin of the different blocks and broken formations. Some components have a Palaeotethyan origin and are characterized by Pennsylvanian and Lower to Middle Permian pelagic and slope deposits. These Palaeotethyan remnants, found exclusively in the Hacialanı mélange, were reworked as major olistostromes in the Neotethys basin during the Eo-Cimmerian orogenic event. Neotethyan elements are represented by Middle Triassic seamounts and by broken formations containing typical Neotethyan conodont faunas such as *Metapolygnathus mersinensis* Kozur & Moix and *M. primitius* s. s., both present in the latest Carnian interval, as well as the occurrence of the middle Norian *Epigondolella praeslovakensis* Kozur, Masset & Moix. Other elements are clearly derived from the former north Anatolian passive margin and are represented by Huğlu-type series including the Upper Triassic syn-rift volcanic event. These sequences attributed to the Huğlu-Pindos back-arc ocean were displaced southward during the Late Cretaceous obduction event. The Tauric elements are represented by Eo-Cimmerian flysch-like and molasse sequences intercalated in Neotethyan series. Additionally, some shallow-water blocks might be derived from the Bolkardağ para-autochthonous and the Taurus-Beydağları marginal sequences.

Key Words: mélange, Triassic, Permian, pelagic, Neotethys, Palaeotethys, Huğlu-Pindos

Güney Türkiye'de Mersin Melanjlarının Jeolojisi ve Korelasyonu

Özet: Makalemizin amacı Mersin ofiyoliti ile ilişkili ofiyolit-altı melanjlarının detaylı bir tasvirini yapmaktır. Mersin melanjlarının hem güney Türkiye'de hem de diğer bölgelerdeki melanj benzeri birlikler veya müşabih serilerle yeni deneştirmelerini teklif ediyoruz. Burada deneştirmelerin paleotektonik anlamları da tartışılmaktadır. En önemli sonuçlar şu şekilde özetlenebilir: Ofiyolit-altı melanjı geç Kretase Sorgun melanjı ve Ladiniyen–Karniyen Hacıalanı melanjı olmak üzere iki birliğe bölünmüştür: Mersin melanjları Antalya ve Mamonia alanları ile birlikte şimdi ana Toros silsilesinin güneyinde bulunan bazı ekzotik birliklerden oluşmaktadırlar ve Güney Taurid Ekzotik Birliklerini karakterize ederler. Bu melanjlarda açıkça muhtelif kırık formasyonların ve blokların karıştığı görülmektedir. Bazı öğeler Paleotetis'den türemişlerdir ve Pensilvaniyen ve erken ve orta Permiyen pelajik yamaç çökellerinden oluşurlar. Bu Paleotetis öğeleri yanızca Hacıalanı melanjında bulunurlar ve Eo-Kimmeriyen orojenik olayı esnasında Neotetis havzasında büyük olistostromlar olarak baştan çökelmişlerdir. Neotetis öğeleri orta Triyas denizaltı tepeleri ve kırık formasyonlarınca temsil edilirler ve en geç Karniyen aralığında bulunan *Metapolygnathus mersinensis* Kozur & Moix ve *M. primitius* s. s. ile orta Noriyen'i temsil eden *Epigondolella praeslovakensis* Kozur, Masset & Moix gibi tipik Neotetis konodontları içerirler. Diğer öğeler içinde açıkça Kuzey Anadolu pasif kenarından türemiş olan ve geç Triyas yaşlı bir riftleşme-yaşıtı volkanik sürecin izlerini taşıyan Huğlu Tepe serisi bulunur. Huğlu-Pindos yay-ardı okyanusuna atfedilen diziler geç Kretase ofiyolit bindirmesi esnasında güneye doğru itilmişlerdir. Taurid serileri, Neotetis serileri içinde tektonik olarak ardalanan Eo-Kimmeriyen fliş benzeri ve molas dizilerinden oluşmaktadırlar. İlâve olarak bazı sığ denizel bloklar Bolkardağ paraotoktonundan ve Toros-Bey Dağları kenar istifinden türemiş olabilirler.

Anahtar Sözcükler: melanj, Triyas, Permiyen, pelajik, Neotetis, Palaeotetis, Huğlu-Pindos

Introduction

The term 'mélange' was first introduced to describe a complicated tectonic mixture in the Precambrian Mona Complex of Anglesey Island in Wales (Greenly 1919). Much later, the term was re-used in Turkey by Bailey & McCallien (Ankara mélanges; 1950, 1953), in Iran by Gansser (coloured mélanges; 1955), and in California by Hsu (Franciscan Complex; 1968). From that time onward, it was broadly applied to different kinds of chaotic complexes throughout the world. However, despite the fact that mélanges are widely distributed geological objects, they have always been subject to controversies regarding their definition, origin, deformation mechanism and tectonic significance (Silver & Beutner 1980; Raymond & Terranova 1984). For the last three decades, the term mélange has been more and more used as a synonym for accretionary sequences when including oceanic remnants ('ophiolitic mélange' of Gansser 1974). More recently, trying to gather in one definition the various existing ones, a new descriptive definition and classification of mélange was given by Raymond (1984): mélanges consist of tectonic or sedimentary assemblages of various kinds of blocks (exotic or not) within a fine-grained matrix; with increasing degree of disorder, the future mélange passes first from a coherent unit to a broken unit, then to a dismembered unit and finally to a mélange.

The advent of the concept of plate tectonics definitively confirmed the importance of the recognition of accretion-related mélanges. We consider the components of ophiolitic mélanges to be derived from both an upper ophiolitic obducting plate and a lower oceanic plate and its connected margin. Thus, besides ophiolitic elements, it may incorporate elements of a magmatic arc and a passive continental margin. Their identification and understanding is crucial, especially in a palaeotectonic and palaeogeographic perspective. Although scenarios can become more complicated, as with the Mersin mélanges, elements of the mélanges should be classified according to this dynamic scheme. Moreover, as the lower plate usually totally disappears during the obduction process, it can only be reconstructed from its elements found in the mélanges. Therefore, because of their key location at active margin boundaries, preserved accretion-related mélanges provide strong constraints on the geological evolution of former oceanic domains and their adjacent margins. In Turkey, the study of mélanges has significantly improved the knowledge of the tectonic evolution of the Tethyan oceans (e.g., Şengör & Yılmaz 1981; Parlak & Robertson 2004; Robertson *et al.* 2006, 2007, 2009).

Our paper aims to give a thorough description of the infra-ophiolitic mélanges associated with the Mersin ophiolite (Parlak 1996; Masset & Moix 2004; Parlak & Robertson 2004). Our work is based on field observations and hundreds of fossil identifications both from blocks of various lithologies and the matrix of the mélanges. We then propose to improve regional correlations of the Mersin mélange with other mélange-like units or similar series, located both in southern Turkey and adjacent regions (e.g,. Cyprus, Greece, and Sicily): the palaeotectonic implications of the correlations are also discussed.

Geological Settings

Since the pioneer work of Şengör & Yılmaz (1981), the internal geometry of the Tethyan domain has been recognized to be characterized by a complex array of plate boundary systems composed of a continuously evolving network of ridges, transforms and subduction zones. Their record of activity is now found, in various states of preservation, mainly along the sutures of the Tethysides, the sites of former Tethyan oceans. Recent geological subdivisions of Turkey based on palaeogeography and plate tectonics were made by Okay & Tüysüz (1999) and Bozkurt & Mittwede (2001). Based on proper terrane definitions and geological descriptions of the main sutures, microcontinental blocks, and oceanic domains, Moix *et al.* (2008a) developed this concept further. Presently, the İzmir-Ankara-Erzincan suture divides Turkey into two main tectonic units, the Pontides and the Taurides-Anatolides platform (Figure 1). In the north, the Pontides comprise the Sakarya, İstanbul, Zonguldak and Rhodope-Strandja zones. South of the suture, the composite Taurides-Anatolides domain is subdivided into the Anatolian and Taurus terranes (Stampfli 2000): the Taurus terrane belonged to Gondwana, at least until Early Permian times, whereas the Anatolian terrane has post-Variscan Eurasian affinities. Moix *et al.* (2008a) introduced the term 'South-Taurides Exotic Units' to describe the exotic elements of the Anatolian terrane now found south of the Taurus terrane (such as the Mersin mélanges and ophiolites), juxtaposing or incorporating them into typical Neotethyan units. To the southeast, a major Tertiary suture zone separates the Taurides-Anatolides composite domain from the peri-Arabian system (Figure 1).

The Mersin mélanges belong to the Mersin Ophiolitic Complex (thereafter MOC). In addition to the mélanges, the MOC also consists of a sub-ophiolitic metamorphic sole and well-developed oceanic ophiolitic series. The three structural elements are represented in the field by numerous tectonic slices. The Mersin ophiolite recognized by Juteau (1980) was accurately described by Parlak (1996) and Parlak *et al.* (1996a, b). The Mersin ophiolite formed in a supra-subduction zone (SSZ) tectonic setting during the Late Cretaceous (Parlak & Delaloye 1996, 1999; Çelik 2008). $^{40}Ar/^{39}Ar$ dates from hornblendes show that the age of cooling below 500 °C of the metamorphic sole ranges from 96.0±0.7 Ma to 91.0±0.8 Ma (Parlak 1996; Parlak & Delaloye 1999; Dilek *et al.* 1999). K/Ar datings on hornblendes indicate ages ranging from 94.0±4 Ma to 101±4 Ma (Thuizat *et al.* 1981) with an average of 93.4±2 Ma (Parlak *et al.* 1995). Diabase dykes cutting the metamorphic sole yielded ages ranging between 89.6±0.7 Ma and 63.8±0.9 Ma (Parlak & Delaloye 1996), 86.3±0.5 Ma (Parlak 1996) and 91.0±0.6 Ma (Dilek *et al.* 1999).

North of Mersin, the youngest sediments transgressing over the ophiolitic mélange are early Ypresian around Namrun (Avşar 1992). In Sorgun and Arslanköy, the youngest sediments above the ophiolite belong to the Burdigalian of the Adana Basin (Ricou *et al*. 1975; Pampal 1984, 1987). The age of the Scaglia-type limestones and the first detrital inputs together with the transgressive Tertiary sediments above the ophiolite allow us to constrain the interval for the final thrusting of the MOC onto the southern Tauric margin. The late Campanian to early Maastrichtian flexuration of this margin is clearly younger than the one recorded along the northern margin of the Anatolian terrane, usually of Turonian age, locally starting already during the Cenomanian and was generally sealed by Maastrichtian sediments (Moix *et al*. 2008a).

The Mersin Mélanges

Introduction and Generalities

We thoroughly investigated the previously poorly-studied Mersin mélanges 30–35 km N/NW away from the coastal town of Erdemli. The area is framed by the villages of Gâvuruçtuğu (N), Poyrazlı and Hacialanı (S) and includes the villages of Sorgun and Toros. The Mersin mélange lies on the Tauric platform and is tectonically overlain by the sub-ophiolitic metamorphic rocks and the ophiolitic suite (Figures 1, 2C, 3 & 4). Geological maps of the

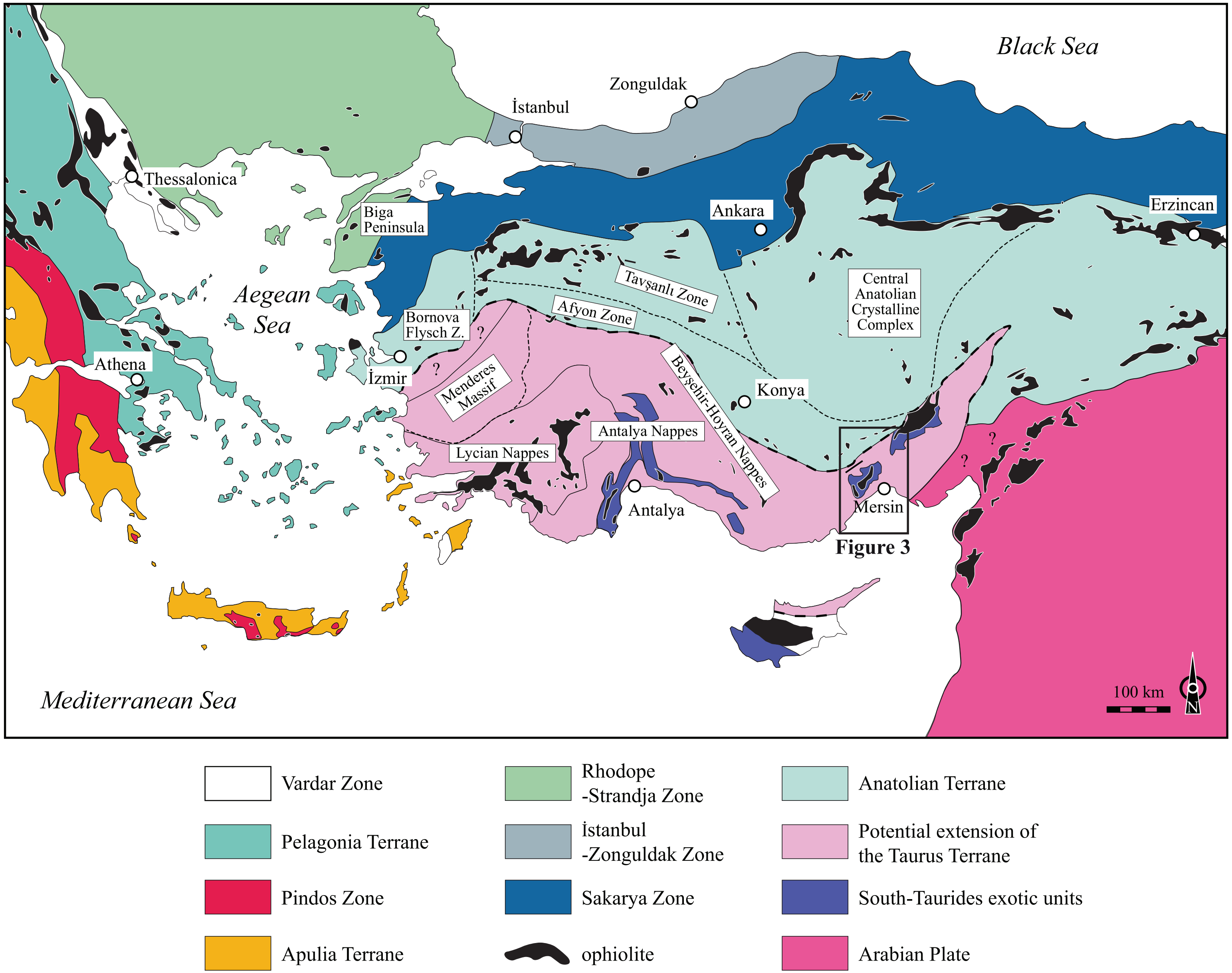

Figure 1. Tectonic map of Turkey and surrounding region. See the explanations in the text. Modified from Moix *et al.* (2008a). Location of Figure 3.

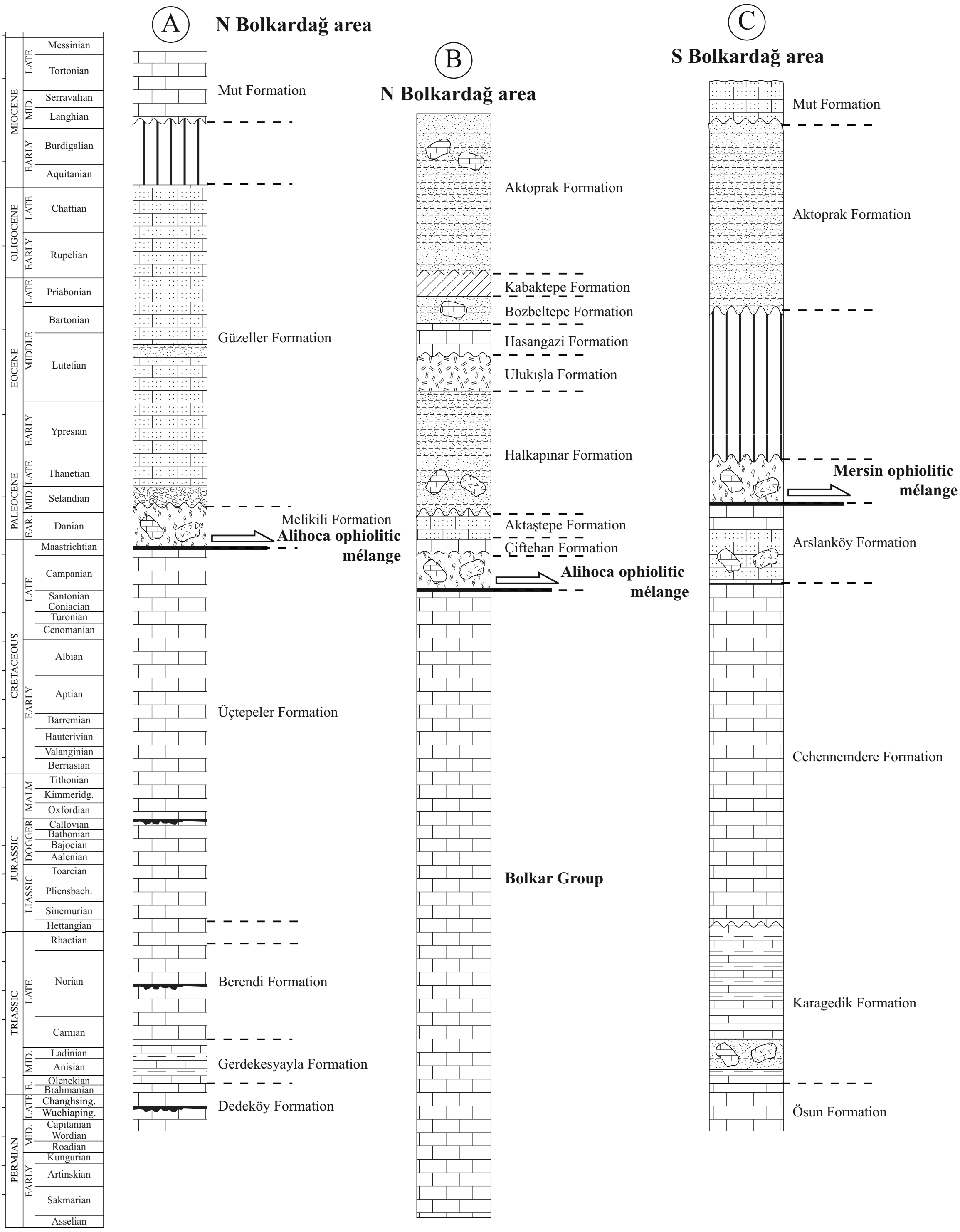

Figure 2. Synthetic lithostratigraphic sections of the paraautochthonous Bolkar Massif north of Mersin. **(A)** Modified from Demirtaşlı *et al.* (1984); **(B)** compiled from Demirtaşlı *et al.* (1984) and Clark & Robertson (2002); **(C)** compiled from Demirtaşlı *et al.* (1984) and Özgül (1984). Key on Figure 6. The geological time scale is after Gradstein *et al.* (2004) for the Early Permian, Jurassic and Cretaceous, and after Kozur (2003a, b) for the Middle–Late Permian and Triassic.

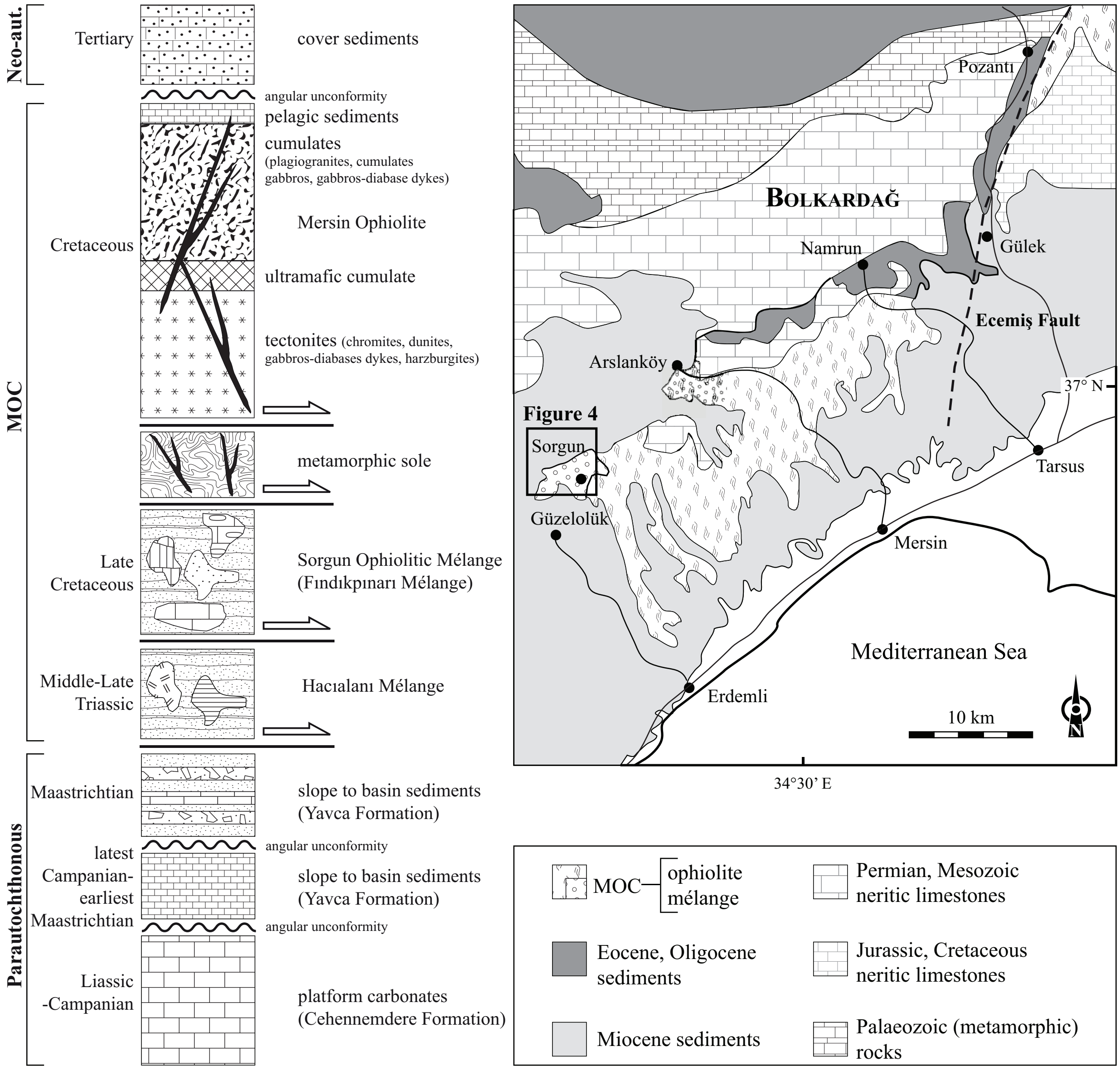

Figure 3. Composite section and simplified geological map of the Mersin Ophiolitic Complex (MOC). Compiled from Parlak (1996), Masset & Moix (2004) and Özer *et al.* (2004). Location of Figure 4.

Mersin ophiolite and associated units were drawn in Arslanköy (Pampal 1984), and in Güzelolük-Sorgun (Pampal 1987). Later, rock assemblages comprising continental margin units, rift series, platform fragments, slabs of metamorphic rocks and fragments of oceanic lithosphere were recognized (Parlak 1996). Four distinctive associations were subsequently identified by Parlak & Robertson (2004): (1) a shallow-water carbonate association; (2) a volcanogenic-terrigenous-pelagic association; (3) a basalt-radiolarite-pelagic limestone association and (4) an ophiolite-derived association.

Because of strong dissimilarities, the Mersin ophiolitic mélange was subdivided into two independent units (Masset & Moix 2004; Moix *et al.* 2007a, b): the first one is the Upper Cretaceous

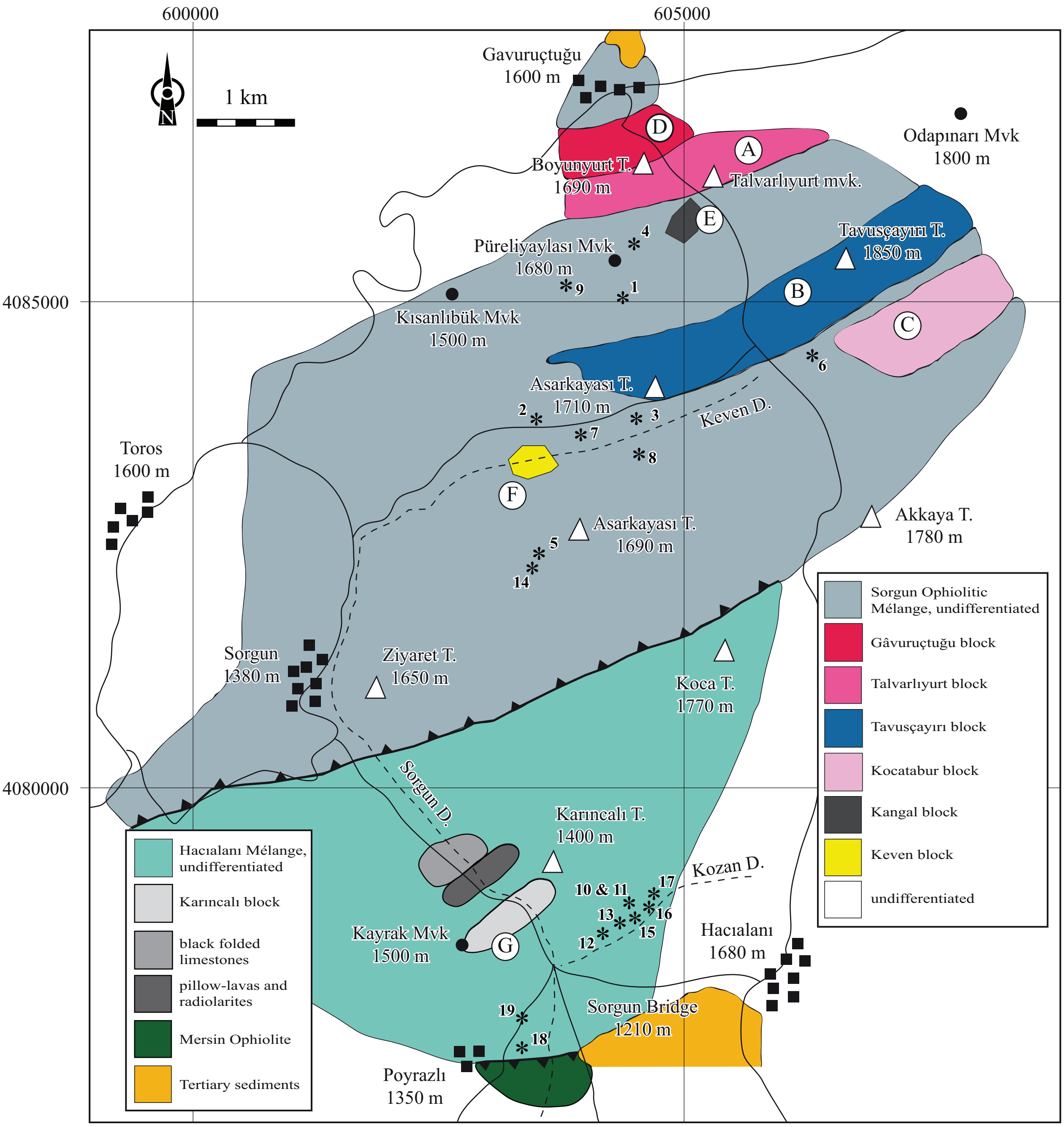

Figure 4. Schematic geological map of the studied area, showing the position of the Sorgun and Hacialanı mélanges after Masset & Moix (2004). Location of the map on Figure 3. Letters refer to sections of Figures 5 & 6. Numbers associated to stars refer to samples presented in Table 1. Coordinates are given in WGS84, UTM Zone 36S.

Sorgun ophiolitic mélange (thereafter SOM), and the second one is the Middle to Upper Triassic Hacialanı mélange (thereafter HM). The distinction between these two mélanges is principally based on field criteria: (1) the presence or absence of ophiolitic material: in the SOM there are large outcrops of serpentinite, gabbros and locally amphibolites, whereas in the HM these lithologies are not

Table 1. Summary of the sample numbers, GPS localities and age of the critical samples described in the text and in the palaeontological plates. Coordinates are given in WGS84, UTM Zone 36S.

	Section		Sample	X-coordinate	Y-coordinate	Age
Sorgun Ophiolitic Mélange	Talvarlıyurt block		C10	605214	4086538	late Oxfordian–Kimmeridgian
			C11	605214	4086538	late Tithonian–Berriasian
			C12	605214	4086538	Berriasian–Hauterivian
			316	606391	4086645	late Barremian–early Aptian
			337	606370	4086576	Cenomanian
	Tavusçayırı block		G4	605728	4084868	Anisian
			G5	605740	4084878	early Carnian
			G7	605787	4084694	late Julian
			G11	606066	4084886	early Tuvalian
			G19	606478	4084743	middle to late Norian
			339	606422	4084593	late Bajocian
	Kocatabur block		MM078	606715	4084592	latest Carnian–earliest Norian
			363	606746	4084529	latest Rhaetian
	Gâvuruçtuğu block		MM030	604596	4086653	middle Norian
	Keven block		M2	603602	4083436	early Asselian
			MM140	603610	4083421	late Early Permian
	1	isolated sample	MM019	604724	4085021	late Turonian–early Coniacian
	2	isolated sample	MM092	603580	4083732	Guadalupian (Midian?)
	3	isolated sample	MM144	604359	4083505	Bashkirian
	4	isolated sample	323	604656	4085693	Early Triassic
	5	isolated sample	353	603723	4082555	late Ladinian
	6	isolated sample	359	606103	4084336	Valanginian–Hauterivian
	7	isolated sample	392	603994	4083325	late Tithonian–early Valanginian
	8	isolated sample	393	604154	4083355	late Serpukhovian–earliest Bashkirian
	9	isolated sample	415	603864	4085197	late Anisian to early Norian
Hacialanı Mélange	Karinkalı block		K5	603160	4078353	Kungurian
	pillow-lavas and radiolarites		J9a	602974	4078792	late Illyrian
			J9b	602974	4078792	latest Illyrian
	Black folded limestones		129/06	602570	4079078	Spathian
	10	isolated sample	MM173	604526	4078836	Guadalupian (Roadian?)
	11	isolated sample	MM174	604526	4078836	Wordian
	12	isolated sample	325	604345	4078575	Middle Permian
	13	isolated sample	329	604516	4078784	Kungurian
	14	isolated sample	355	603588	4082755	Early Permian
	15	isolated sample	378	604434	4078641	Capitanian
	16	isolated sample	383	604522	4078771	Kungurian
	17	isolated sample	384	604535	4078795	late Wordian
	18	isolated sample	J2	603662	4077221	Valanginian
	19	isolated sample	MM157	603637	4077403	Dogger (post-Aalenian, Bajocian?)

represented; (2) the type of lithologies: thick series of pelagic cherts (sometimes associated with tuffites) and calciturbidites, pillow-lavas associated with radiolarian cherts, black folded platy limestones and Upper Triassic turbiditic sandstones are restricted to the HM. After processing the collected samples, the age and the palaeontological affinity of the components of the mélanges (the core of the present paper), the Colour Alteration Index of the conodonts (CAI) and the Thermal Alteration Index (TAI) of the pollens gave additional clues to validate the subdivision into these two units. The CAI and TAI indicate the grade of metamorphism (Epstein *et al.* 1977; Rejebian *et al.* 1987): CAI values in the SOM are 1 (50–80 °C) and between 3 and 4 for the HM (200–250 °C); TAI values in the matrix of the SOM are 0% R_o for Late Jurassic–Cretaceous rocks, effectively no thermal alteration. In contrast, Middle to Upper Triassic rocks from the HM gave 0.7% R_o, corresponding to a thermal alteration at about 200 °C.

In places, the mélanges consist of a chaotic accumulation of blocks and rocks in a tectonic and sedimentary mixture (olistostrome) of clastics, ophiolitic material, and oceanic and exotic blocks of various ages. Blocks in the mélanges typically range in size from metres to hundreds of metres. Broken formations are represented by elongated bodies ranging in size from hundreds of metres to kilometres. Systematic dip and strike measurements indicate that the final emplacement of the MOC and the reorganization of the blocks and broken formations follow a northeast–southwest trend, characterized by a moderate to steep north-westward or south-eastward dips. Tight to isoclinal folds, north verging C-S fabrics and duplex structures, verge normally northward, as in the upper part of Keven Deresi, NE of Sorgun (Figure 4), where many slices of serpentinite exhibit northward vergence. In contrast, south-verging slices of limestone, mainly striking northeast–southwest, can be observed near Asarkayası Tepe, NNE of Sorgun (Figure 4). According to Parlak *et al.* (1996a), the metamorphic sole can be used as evidence of thrusting from the southeast to the northwest in present-day geographic coordinates. However, structural analysis on metamorphic soles can only bring information on the former intra-oceanic obduction processes. Finally Parlak & Robertson (2004) proposed a northward obduction of the Mersin ophiolite onto the Tauric carbonate platform.

The Parautochthonous Sequence and the Transition to the Mersin Ophiolitic Complex

The Bolkardağ belongs to the Taurus terrane sensu Moix *et al.* (2008a) and is the parautochthon for the Alihoca and the Mersin ophiolites (Figure 2A–C). This massif was seen as a window of the Arabian plate and formed the so-called 'Calcareous Axis' (Ricou *et al.* 1975). On a regional scale, the Bolkar Group is divided into two major thrust sheets, namely the northern and southern Bolkardağ units, separated by the Koşan overthrust. The northern Bolkardağ unit consists of a partly metamorphosed to greenschist facies Permian to Upper Cretaceous thick platform-type sequence (Figure 2A, B), locally cut by diabase intrusions. The upper part of the Maastrichtian Üçtepeler formation is composed of grey pelagic limestone and shortly predates the setting of the Alihoca ophiolitic mélange, itself sealed by upper Palaeocene limestones (Demirtaşlı *et al.* 1984). The southern Bolkardağ unit is also a Permian to upper Cretaceous thick platform-type series (Figure 2C). The upper part of the platform shows a continental flexuration during the Campanian (Cehennemdere formation) followed by a upper Campanian–Maastrichtian flysch, including ophiolitic olistostromes and olistoliths (Arslanköy formation). An ophiolitic mélange lies tectonically above the Arslanköy formation, in turn unconformably overlain by the Upper Eocene to Oligocene Aktoprak and the Middle Miocene Mut formations (Demirtaşlı *et al.* 1984).

The transition between the Bolkardağ and the Mersin ophiolite was described near Arslanköy by Ricou *et al.* (1975) and later investigated in the Mersin-Arslanköy-Yavca area (Özer *et al.* 2004; Parlak & Robertson 2004; Taşlı *et al.* 2006). According to Ricou *et al.* (1975), the calcareous sequence plunges southwards, and is capped by limestones rich in rudist remains. They are then overlain by a few metres of thin-bedded red limestone with *Globotruncana arca* (Cushman), *G. calciformis* Vogler, *G.* ex gr. *stuarti* (de Lapparent) and *Orbitoides media* d'Archiac, *Siderolites calcitrapoides* Lamarck, yielding a Maastrichtian age. Finally, these levels are in turn overlain by 25 m of greenish, azoic thin-bedded sandstones. We also logged near Arslanköy a sedimentary succession from the platform to the trench (flexural basin), which confirms the previous work. An assemblage just below the sandstones yielded *Globotruncana bulloides* Vogler, *G. linneiana* (d'Orbigny), *Globotruncanita stuartiformis* (Dalbiez), *G. stuartiformis* aff. *calcarata* and *Inoceramus* sp., showing that the Scaglia limestone was deposited during the late Campanian–earliest Maastrichtian interval. The facies transition represents the latest stage of Cretaceous (Campanian–Maastrichtian) neritic sedimentation before the flexuration of the margin and the obduction of the ophiolites onto the southern margin of the Taurus terrane.

The Sorgun Ophiolitic Mélange (SOM)

The SOM occupies the highest tectonic position and is found in the northern part of the investigated area. As the SOM is analogous to the Fındıkpınarı formation (Özer *et al*. 2004), and to the mélange described in Arslanköy (Demirtaşlı *et al*. 1984), it should be laterally extensive. The SOM is delimited to the north by the transgressive rocks of Cenozoic age and to the south by the HM. Many coherent series with kilometric lateral extent were identified within the SOM, and we consider the Gâvuruçtuğu, Talvarlıyurt, Tavusçayırı and Kocatabur blocks as broken formations or nappes (Figures 4 & 5A–D). In addition to these kilometric blocks, there is a multitude of smaller blocks: carbonates ranging from Early Carboniferous to Late Triassic; radiolarites ranging from Ladinian to late Turonian–early Coniacian; rare blocks of amphibolites; blocks of partially serpentinous peridotites, gabbros and pillow-lavas, and blocks of debris-flows (including sometimes ophiolitic debris). Within these small-scale blocks, some are of particular interest as they exhibit peculiar lithologies, such as the Kangal, Zindan, Keven, Gerdemelipinarı, Fırıntaş, Çardak and Değırmenbaşı blocks (Figure 6E).

Matrix and Blocks of the Sorgun Ophiolitic Mélange– The matrix of the SOM corresponds partly to the Cenomanian to Santonian–Campanian Başpınar formation (Pampal 1987), which contains deep sea radiolarites, pelagic limestones and ophiolite-derived rocks. This formation is well-exposed near Toros. The ductile fraction of the SOM matrix is generally serpentinitic or argillitic (pelitic rocks). In places, it is composed of sheared serpentinites, in which massive serpentinite blocks up to several metres across are embedded. This type of matrix is exposed in the upper part of the ENE–WSW-trending Keven Deresi (Figure 4) where the sheared serpentinites present small-scale folds and faults. Elsewhere, the matrix is composed of mass- and debris-flows rich in ophiolitic material, lavas and radiolarites. Blocks of radiolarites within the debris-flows show boudins indicating maximal elongation on an approximately NW–SE axis. Locally, the matrix comprises strongly foliated greenish fine- to coarse-grained sandstones and mudstones.

Several types of facies are found floating within the matrix. Near Sorgun, neritic limestone units are structurally repeated several times, with a soft and fine-grained tuffitic matrix in between. Within the SOM, most of the blocks are made of Upper Triassic massive neritic limestones containing the following taxa: *Palaeolituonella meridionalis* (Luperto), *Aulotortus sinuosus* Weynschenk, *A*. sp., *Endothyra tyrrhenica* Vachard, Martini, Rettori & Zaninetti, *Glomospirella* sp., *Ophthalmidium* sp., *Endoteba* sp., *Reophax* sp. and abundant Duostominidae were identified in several blocks. In Keven Deresi, the first occurrence of Carboniferous limestones in the Mersin mélanges is illustrated by blocks of medium-bedded black fetid bioclastic wackestones which yielded late Serpukhovian–earliest Bashkirian (Sample 393, Table 1, Figure 4) and Bashkirian ages. The late Serpukhovian–earliest Bashkirian assemblage is composed of microbialitic biopelmicrites (thrombolites) with *Terebella* (worm burrows) (Plate 1, Figure 2), dendrolites of the pseudo-alga *Praedonezella* cf. *cespeformis* Kulik (Plate 1, Figure 1), another pseudo-alga *Stacheoides* sp., ostracods, and the foraminifera *Hemithurammina fimbriata* (Howchin) emend. Mamet, *Eotuberitina reitlingerae* Miklukho-Maklay, *Diplosphaerina* sp., *Tuberitina bulbacea* Galloway & Harlton, *Earlandia elegans* (Rauzer-Chernousova & Reitlinger in Rauzer-Chernousova & Fursenko), *Endothyra* sp., *Pseudotaxis* (= *Endotaxis*) *brazhnikovae* (Bogush & Juferev), *Tetrataxis* sp., *Plectostaffella* cf. *varvariensiformis* Brazhnikova & Vdovenko (Plate 1, Figure 3) and *Globivalvulina* aff. *moderata* Reitlinger. In microfacies, the Bashkirian assemblage (Sample MM144, Table 1, Figure 4) comprises metazoan fragments such as brachiopods (tests and spines), bryozoans, ostracods, gastropods, sponge spicules (monaxones and polyaxones), conodonts, crinoids, corals; pseudo-algae: *Anthracoporellopsis machaevii* Maslov (Plate 1, Figure 6a), *Stacheoides*? sp.; foraminifera: *Pachysphaerina pachysphaerica* (Pronina), *Hemithurammina fimbriata* (Howchin) emend. Mamet (Plate 1, Figure 7), *Eotuberitina reitlingerae*

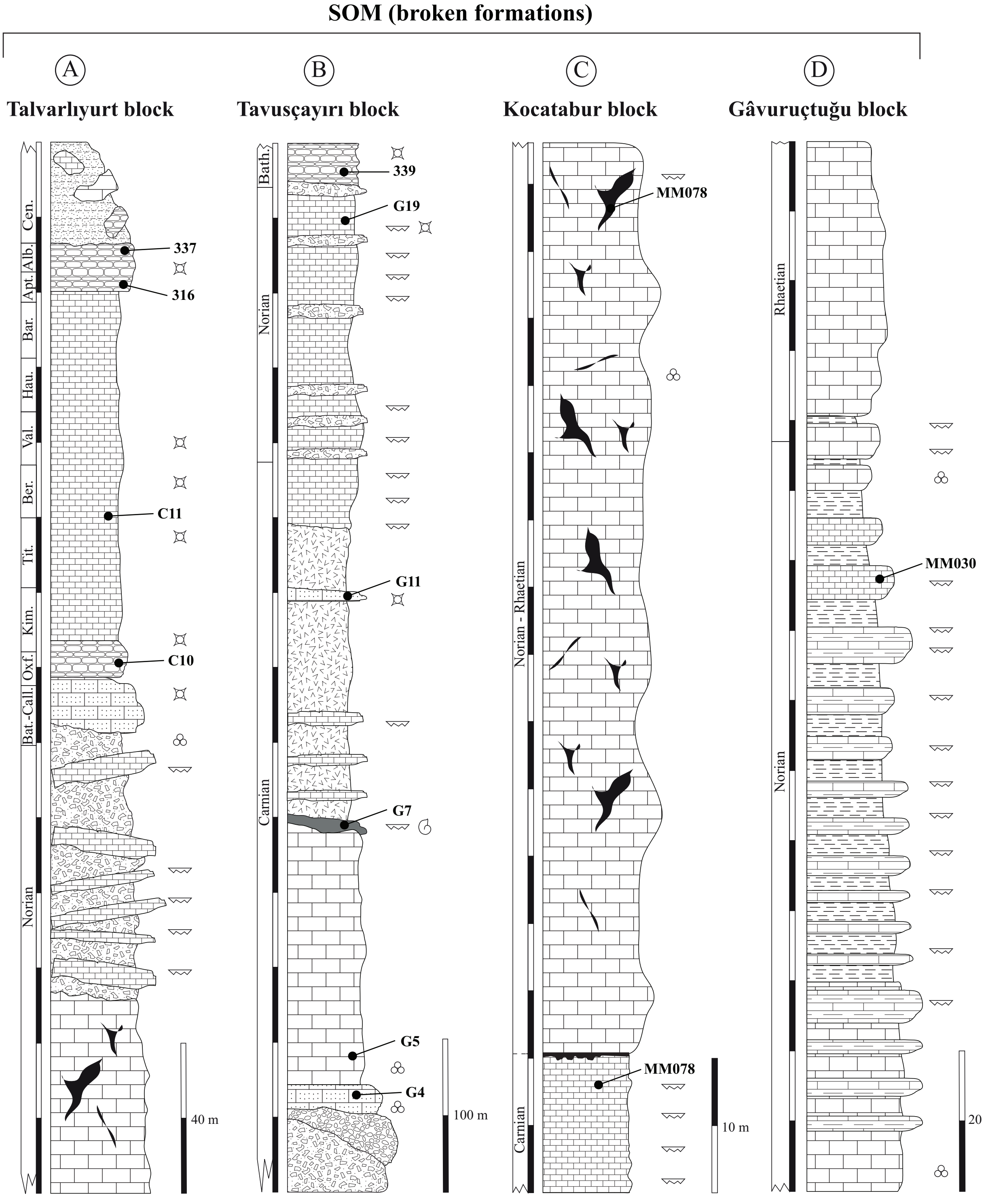

Figure 5. Synthetic lithostratigraphic sections of the broken formations in the Sorgun Ophiolitic Mélange. Location of the logs on Figure 4 and key on Figure 6.

Miklukho-Maklay, *Tuberitina* sp., *Asteroarchaediscus postrugosus* (Reitlinger) (Plate 1, Figure 4), *Eolasiodiscus transitorius* Brazhnikova & Yartseva, *Earlandia* sp., *Endothyra* sp., *Iriclinella spirilliniformis* (Brazhnikova & Potievskaya) (Plate 1, Figure 8), *Tetrataxis* sp., *Globivalvulina moderata* Reitlinger, *G. bulloides* (Brady), *Eostaffella pseudostruvei* Rauzer-Chernousova & Belyaev in Rauzer-Chernousova *et al., Ozawainella* aff. *digitalis* Manukalova (Plate 1, Figure 7), *Calcivertella* sp., *Calcitornella* sp., and *Cornuspira multivoluta* (Reitlinger) (Plate 1, Figures 5 & 6b, c). This facies seems widespread in the Taurides (Brinkmann 1976; Altıner 1981; Lys 1986). Another block of lithoclastic rudstone presents a reworking of different Bashkirian, Moscovian, Kasimovian, Gzhelian and Permian (probably Midian) facies and microfossils (Sample MM092, Table 1, Figure 4), including algae *sensu lato* such as *Archaeolithoporella hidensis* Endô (Plate 1, Figures 17, 18b), *Tubiphytes obscurus* Maslov (Plate 1, Figure 18a), *Koivaella permiensis* Chuvashov, *Praedonezella cespeformis* Kulik, *Beresella* sp. (Plate 1, Figure 16), *Ungdarella* ex gr. *uralica* Maslov (Plate 1, Figure 12b), the foraminifera *Pachysphaerina pachysphaerica* (Pronina), *Eotuberitina reitlingerae* Miklukho-Maklay, *Earlandia* sp., *Iriclinella* sp. (Plate 1, Figure 12a), *Obsoletes* sp. (Plate 1, Figure 10), *Nankinella* sp., *Pseudostaffella* ex gr. *antiqua* (Dutkevich) (associated with and dating all the big oolites (Plate 1, Figure 13) occasionally isolated in the microfacies), *Profusulinella* sp., *Fusulinella* sp. (Plate 1, Figure 9), *Tetrataxis* sp., *Charliella* sp., *Rauserites* sp. (Plate 1, Figure 15), *Bradyina lucida* Morozova emend. Pinard & Mamet (Plate 1, Figure 14), and *Asteroarchaediscus baschkiricus* (Krestovnikov & Teodorovich) (Plate 1, Figure 11). Abundant pelagic blocks are mainly represented by Hallstatt Limestone facies. A micro-conglomerate (Sample 323, Table 1, Figure 4) reworks basal Triassic clasts including the conodonts *Hindeodus parvus* (Kozur & Pjatakova), *H. parvus anterodentatus* Kozur, *Ellisonia transita* nomen nudum, *Hadrodontina* sp. and *Clarkina carinata* (Clark), plus Capitanian pebbles characterized by *Archaeolithoporella hidensis* Endô and Lopingian pebbles characterized by *Paradoxiella* sp. Pelagic facies belonging to the *Hindeodus parvus* Zone are not common in Turkey and *H. parvus* was so far only discovered in the Antalya Nappes (Crasquin-Soleau *et al*. 2002). Between Kısanlıbük Mvk. and Püreliyaylası Mvk. (Figure 4), the conodonts *Paragondolella excelsa* Mosher, *P. noah* (Hayashi) and *Epigondolella orchardi* Kozur were identified within a few centimetres of a upper Anisian to lower Norian highly condensed succession of pelagic Hallstatt Limestones (Sample 415, Table 1, Figure 4). These limestones unconformably overlie shallow-water limestones rich in corals presenting a palaeo-reef development. This condensed series might have been deposited on a Neotethyan seamount.

Radiolarites are very common and range from Middle Triassic to Coniacian, suggesting that at least one deep open basin remained open until this time interval. Infrequent outcrops of typical Upper Triassic turbiditic sandstones with plants, associated with *Halobia*-bearing limestones were recognized. One sample of green folded radiolarian chert (Sample 353, Table 1, Figure 4) yielded a late Ladinian association composed of *Pseudostylosphaera* spp. (Plate 2, Figure A) and *Muelleritortis* spp. (Plate 2, Figure B). The youngest identified sediment is a upper Turonian–lower Coniacian radiolarian chert (Sample MM019, Table 1, Figure 4), characterized by *Cryptamphorella* spp., *Archaeodictyomitra* sp. (Plate 2, Figure F), *Dictyomitra* spp. (Plate 2, Figures E, G & J), *D. formosa* Squinabol (Plate 2, Figure Q), *D. koslovae* Foreman (Plate 2, Figures H, K, L, M, O & P), *Pseudodictyomitra* aff. *pseudomacrocephala* (Squinabol) (Plate 2, Figures D, N), *Holocryptocapsa cryptodon* Dumitrică (Plate 2, Figure I) and *Xitus* cf. *mclaughlini* (Pessagno) (Plate 2, Figure C). A Valanginian–Hauterivian association from a radiolarian chert (Sample 359, Table 1, Figure 4) is characterized by *Archaeodictyomitra apiarium* (Rüst), *A. coniforma* Dumitrică, *Cinguloturris cylindra* Kemkin & Rudenko and *Pantanellium squinaboli* (Tan). An upper Tithonian–lower Valanginian radiolarian chert (Sample 392, Table 1, Figure 4) yielded *Archaeodictyomitra excellens* (Tan), *Cinguloturris cylindra* Kemkin & Rudenko, *Emiluvia chica* Foreman, *E. pessagnoi* Foreman, *Loopus yangi* Dumitrică, *Mirifusus dianae* (Karrer), *Obesacapsula cetia* (Foreman), *Parapodocapsa furcata* Steiger, *Triactoma tithonianum* Rüst, *Tritrabs casmaliaensis* (Pessagno) and *Syringocapsa* sp. A Valanginian chert was also discovered in the HM, immediately below the Mersin ophiolite.

Broken Formations of the Sorgun Ophiolitic Mélange– The Talvarlıyurt block (Figures 4 & 5A, Table 1) is a 300-m-thick sequence with a moderate lateral extent. Its lithological components are sometimes reproduced on a smaller scale in the SOM. The sequence begins with grey neritic massive limestones (Late Triassic?), followed by medium-bedded limestones with replacement cherts. Several mass-flows (100 m) mark a transition from neritic to deeper environments. These gravity flows rework complete metre-scale stratigraphic successions of shallow water, slope and deep marine sediments. Thin-bedded grey to pink micritic nodular limestones with replacement cherts yielded a fauna characterized by bivalves, conodonts, sponge spicules, ostracods and radiolaria of late early Norian age. Hallstatt Limestone yielded middle Norian conodonts. Another block yielded Middle to Late Triassic shallow water fauna, whilst another gave a basal Norian age in pelagic facies. The matrix of these mass-flows is a red micrite forming dyke-like structures, interpreted as the signature of a Late Triassic 'Neotethyan' rifting (Parlak 1996; Parlak & Robertson 2004). Above these large reworked blocks, a mega-breccia already recognized by Parlak & Robertson (2004) comprises cm- to m-scale elements of pink, grey and mauve micritic limestones, red siliceous limestones, red cherts and black cherts enveloped in a pink arenitic to micritic matrix. The uneven surface of the breccia is locally filled by a red, partly silicified calcarenite which yielded Bathonian–Callovian radiolaria.

The sequence continues with thin-bedded reddish to brown radiolarites ranging from late Oxfordian to Kimmeridgian (Sample C10, Table 1, Figure 5A). The assemblage yielded *Emiluvia orea* Baumgartner, transitional to *E. ultima* Baumgartner & Dumitrică, *Hexasaturnalis minor* (Baumgartner), *H. nakasekoi* Dumitrică & Dumitrică-Jud, *Higumastra* sp., *Podobursa spinosa* Ožvoldova, *P.* sp., *Tripocyclia* cf. *jonesi* Pessagno, *Angulobracchia biordinalis* Ožvoldova, *Archaeodictyomitra apiarium* (Rüst), *A. excellens* (Tan), *A. minoensis* (Mizutani), *Pantanellium* cf. *squinaboli* (Tan), *Tetratrabs bulbosa* Baumgartner, and *Zhamoidellum ovum* Dumitrică. This radiolaritic interval is followed by Majolica-type facies which consists of 100 m of very thin- to thin-bedded mauve, pink, grey and green micritic siliceous and argillaceous platy limestones. These limestones are rich in primary cherts, which form discontinuous layers and nodules containing radiolaria of late Tithonian to Berriasian age in the lower part (Sample C11, Table 1, Figure 5A). The assemblage comprises *Angulobracchia portmanni* Baumgartner, *Dicerosaturnalis dicranacanthos* (Squinabol), *Emiluvia chica* Foreman, *Pantanellium squinaboli* (Tan), *Parvicingula* sp., *Ristola altissima* (Rüst), *Svinitzium depressum* (Baumgartner) and *Tetratrabs*? *radix* Jud. Nodules in the upper part yielded the following Berriasian–Hauterivian taxa (Sample C12, Table 1, Figure 5A): *Hemicryptocapsa* cf. *capita* Tan, *Pantanellium aduncum* (Parona), *P. squinaboli* (Tan) and *Syringocapsa agolarium* Foreman. It continues with 30 m of red to brownish radiolarites ranging in age from late Barremian/early Aptian (Sample 316, Table 1, Figure 5A) in the lower part, to Cenomanian in the upper part (Sample 337, Table 1, Figure 5A). The lower assemblage includes *Acaeniotyle diaphorogona* Foreman, *Archaeodictyomitra excellens* (Tan), *Aurisaturnalis carinatus perforatus* Dumitrică & Dumitrică-Jud, *Dicerosaturnalis amissus* (Squinabol), *Dictyomitra communis* (Squinabol) (Plate 2, Figures U, Y, AA & AB), *Hiscocapsa asseni* (Tan) (Plate 2, Figure V), *Praexitus alievi* (Foreman) (Plate 2, Figure R), *Pseudodictyomitra carpatica* (Lozinyak) (Plate 2, Figure X), *P. lilyae* (Tan) (Plate 2, Figure Z), *P.* cf. *thurowi* Dumitrică (Plate 2, Figure AC), *Pseudoeucyrtis zhamoidai* (Foreman) (Plate 2, Figure W), *P. tenuis* (Rüst), *Suna hybum* (Foreman) (Plate 2, Figure S), *Thanarla pacifica* Nakaseko & Nishimura and *Xitus vermiculatus* (Renz) (Plate 2, Figure T). The upper assemblage is characterized by *Pseudodictyomitra pseudomacrocephala* (Squinabol) and *P.* cf. *tiara* (Holmes). The sequence ends with a wildflysch including metre- to tens of metres-scale blocks enveloped in a turbiditic sandstones matrix.

The Tavusçayırı block (Figures 4 & 5B, Table 1) is an isolated 600-m-thick broken formation. Its lateral extent is large (km-scale), and its lithological components are sometimes reproduced on a smaller scale elsewhere in the mélange. This succession represents a typical transgressive sequence marking the break-up of a platform and the opening of a rift basin in Late Triassic times. The sequence starts with 15–20 m of polymict breccia in a red micritic matrix. The elements are heterogeneous in size, varying from mm- to m-size and are mostly composed of white neritic limestones, pink micritic limestones and red calcarenites. Some elements yielded Middle Triassic pelagic faunas. Above an erosional contact, the breccia is followed by 60 m of polygenic clast-supported conglomerate with a red silty matrix. The conglomerate shows cross-bedding and is composed by cm- to dm-size elements, such as black and white, partly reefal limestones, beige and red micritic limestones, and sandstones. This conglomerate is interpreted to be the product of the dismantling of a platform. It is followed by 15 m of black calciturbidites (Sample G4, Table 1, Figure 5B), reworking foraminifers, corals (Permian?), algae and megalodontid-type bivalves. The foraminifera *Gaudryina* sp., *Pilaminella* sp., *Pilammina densa* Pantić and *Ophthalmidium ubeyliense* Dager are characteristic of the Middle–Late Triassic interval, whereas *Pilammina densa* indicates precisely the Anisian.

The series continues with a brownish medium-bedded wackestone (Sample G5, Table 1, Figure 5B), containing echinoderms, ostracods and the foraminifera *Pilammina densa* Pantić, *Hoyenella inconstans* (Michalik, Jendrejacova & Borza), *Ophthalmidium* sp. and *Cucurbita* sp., plus Duostominidae indicating a Carnian to Rhaetian age; because of the age of the overlying beds, an early Carnian age is indicated for these deposits. This type of foraminiferal association is typical for reef environments and is comparable to assemblages described in Cyprus by Martini *et al.* (2009). The platform ends with an irregular surface made of reef limestones showing syn-sedimentary faulting. The palaeo-surface is covered by discontinuous pink micritic nodular limestones in Hallstatt Limestone facies (Sample G7, Table 1, Figure 5B) which yielded ammonoids, foraminifera, echinoderms, crinoids, fish remains, brachiopods and conodonts of middle Carnian age. The association, characteristic of the late Julian *Trachyceras austriacum* Zone, includes *Joannites cymbiformis* (Wulfen), *J.* sp., *Megaphyllites jarbas* (Münster), *Coroceras* sp., *Neoprotrachyceras*? sp. and *Sirenites* cf. *senticosus* (Dittmar). Near Tavusçayırı Tepe in the SOM, these levels were erroneously assigned to the Early Jurassic by Parlak & Robertson (2004).

On our reference section, the Hallstatt Limestone is conformably overlain by 130 m of thin-bedded Huğlu-type redeposited green tuffites showing flute-casts, load-casts and also Bouma sequences. The geochemical signature is of arc-type (VAB), suggesting possible derivation from an eroding arc. The thickness of these deposits is variable from one section to another, and they may be associated with highly altered brownish lavas and tuffs cut by numerous faults, outlined by fluid circulations. The tuffites may have acted as a preferential level for inter-slicing or thrusting. The tuffitic series is interspersed with alternations of micritic limestones and calciturbidites. One micritic limestone level (Sample G11, Table 1, Figure 5B) contains conodonts, sponge spicules, ostracods and a well-preserved radiolarian fauna of the early Tuvalian *Spongotortilispinus moixi* Zone (Kozur *et al.* 2007a, b, c, 2009; Moix *et al.* 2007b). The tuffitic episode is followed by 300 m alternating pelagic limestones, calciturbidites, bioclastic limestones and debris-flows. The pelagic limestone sedimentation starts usually during the upper Carnian, continues during the Norian where some parts could be omitted and most probably ends during the early Rhaetian (?). One yellow nodule (Sample G19, Table 1, Figure 5B) within these pelagic limestones yielded a few specimens of *Annulotriassocampe* spp. (Plate 3, Figure A) and ?*Livarella densiporata* Kozur & Mostler (Plate 3, Figure B). According to this assemblage and to the general succession, the age is most probably middle to late Norian. However, the isolated Değirmenbaşı block shows that tuff deposition persisted at least until the early Norian. In places, a Toarcian Ammonitico Rosso Limestone containing the genera *Hildoceras*, *Porpoceras* and *Calliphylloceras* is well-developed. The early Rhaetian (?) limestones are overlain by a breccia, followed by late Bajocian brownish radiolarian cherts (Sample 339, Table 1, Figure 5B) composed of *Archaeospongoprunum imlayi* Pessagno (Plate 3, Figures C, I), *Homoeoparonaella* cf. *argolidensis* Baumgartner, *Mirifusus fragilis praeguadalupensis* Baumgartner & Bartolini, *Paronaella broennimanni*

Pessagno (Plate 3, Figure F), *Protunuma costata* (Heitzer) (Plate 3, Figure H), *Stichocapsa robusta* Matsuoka, *Teichertus splendidus* Hull, *Transhsuum maxwelli* (Pessagno) (Plate 3, Figure E), *T. medium* Takemura (Plate 3, Figure D), *Tricolocapsa conexa* Matsuoka, *Tritrabs casmaliaensis* (Pessagno) and *Napora* sp. (Plate 3, Figure G). This radiolarian interval corresponds to the Early–Middle Jurassic radiolarites reported by Kozur (1997) in the Huğlu type area.

The Kocatabur block (Figures 4 & 5C, Table 1) is about 100 m thick and is situated south of the Tavusçayırı block. The lateral extent of this broken formation is relatively large (km-scale) and its lithological components are reproduced at lower-scale elsewhere in the SOM. The sequence begins with 4 m of thin-bedded grey to pink micritic and nodular limestones. The fauna is composed of sponge spicules, foraminifera, fish remains, ammonoids and conodonts, which give a latest Carnian to earliest Norian age for the pelagic sequence (Sample MM078, Table 1, Figure 5C). It is notably rich in *Metapolygnathus mersinensis* Kozur & Moix and *M. primitius* s. s., both good indicators of the Neotethyan domain (Moix *et al.* 2007b). It continues with 100 m of recrystallized massive limestones. The presence of fissure fillings indicates the fracturing of the platform during the Late Triassic. These neptunian dykes (Sample 363, Table 1, Figure 5C) are composed of red micrite rich in brachiopods, bivalves, gastropods, echinoderms and pelagic conodonts indicative of the latest Rhaetian *Misikella ultima* Zone.

The Gâvuruçtuğu block (Figures 4 & 5D, Table 1) is a 200-m-thick sequence with a moderate lateral extent. This type of facies seems to be unique in the SOM. The sequence begins with 30 m of medium-bedded grey to brownish fetid micritic limestones of Norian age. The presence of organic matter and framboidal pyrite, a common diagenetic phase in many types of shale, is especially abundant in strata formed under oxygen-poor depositional conditions indicate an anaerobic environment (Wilkin & Barnes 1997; Wignall *et al.* 2005). The fauna consists of fish remains, foraminifera, gastropods, bivalves, radiolaria and sponge spicules, all characteristic of a (restricted) basinal or ramp environment. The overlying sequence is transitional to grey micritic limestones of middle Norian age, above which there is a facies change to 80 m of thin- to medium-bedded black to grey micritic argillaceous limestones alternating with marls. Foraminifera, fish remains, brachiopods, ostracods, echinoderms, nautiloids and conodonts are present, but rare. A middle Norian age for the first layers and a late Norian age 30 m above have been determined. 4 m of brownish and recrystallized limestones alternating with marls mark the transition to highly recrystallized massive grey limestones with replacement cherts. Based on foraminifera, the uppermost levels gave a Late Triassic age. Locally, these limestones are folded, with rare medium- to large-scale southward verging tight to isoclinal folds.

The Gâvuruçtuğu block is characterized by a conodont fauna with middle Norian guide forms (Sample MM030, Table 1, Figure 5D), such as *Mockina postera* (Kozur & Mostler), but above all with *Epigondolella praeslovakensis* Kozur, Masset and Moix (Moix *et al.* 2007b). This latter species has so far only been found in the Neotethys and adjacent areas with unrestricted connection to the Neotethyan fauna (e.g., Roghi *et al.* 1995). *Epigondolella praeslovakensis* was so far assigned to *Mockina slovakensis* (Kozur), but Roghi *et al.* (1995) found in Carnia a phylomorphogenetic lineage from transitional forms *E. praeslovakensis* - *M. slovakensis* into typical *M. slovakensis*. The data of Roghi *et al.* (1995) are hence important for the palaeogeographic evaluation because they indicate the occurrence of *E. praeslovakensis* in the middle Norian of the Neotethys, a time interval so far rarely investigated for conodonts. The Neotethyan character of the middle Norian conodont fauna of the Gâvuruçtuğu block indicates a derivation from the south, i.e. the Neotethyan margin of this block. The occurrence of *E. praeslovakensis* suggests the Talvarlıyurt block should also have a Neotethyan origin, but *E. praeslovakensis* is very rare in this block for facies-related reasons (more open marine development).

The Kangal block (Figures 4 & 6E) exhibits a pelagic sequence which ranges from the late Carnian to the late early Norian. This 80-m-thick block comprises at its base thin- to medium-bedded grey to pink micritic limestones of Hallstatt Limestone

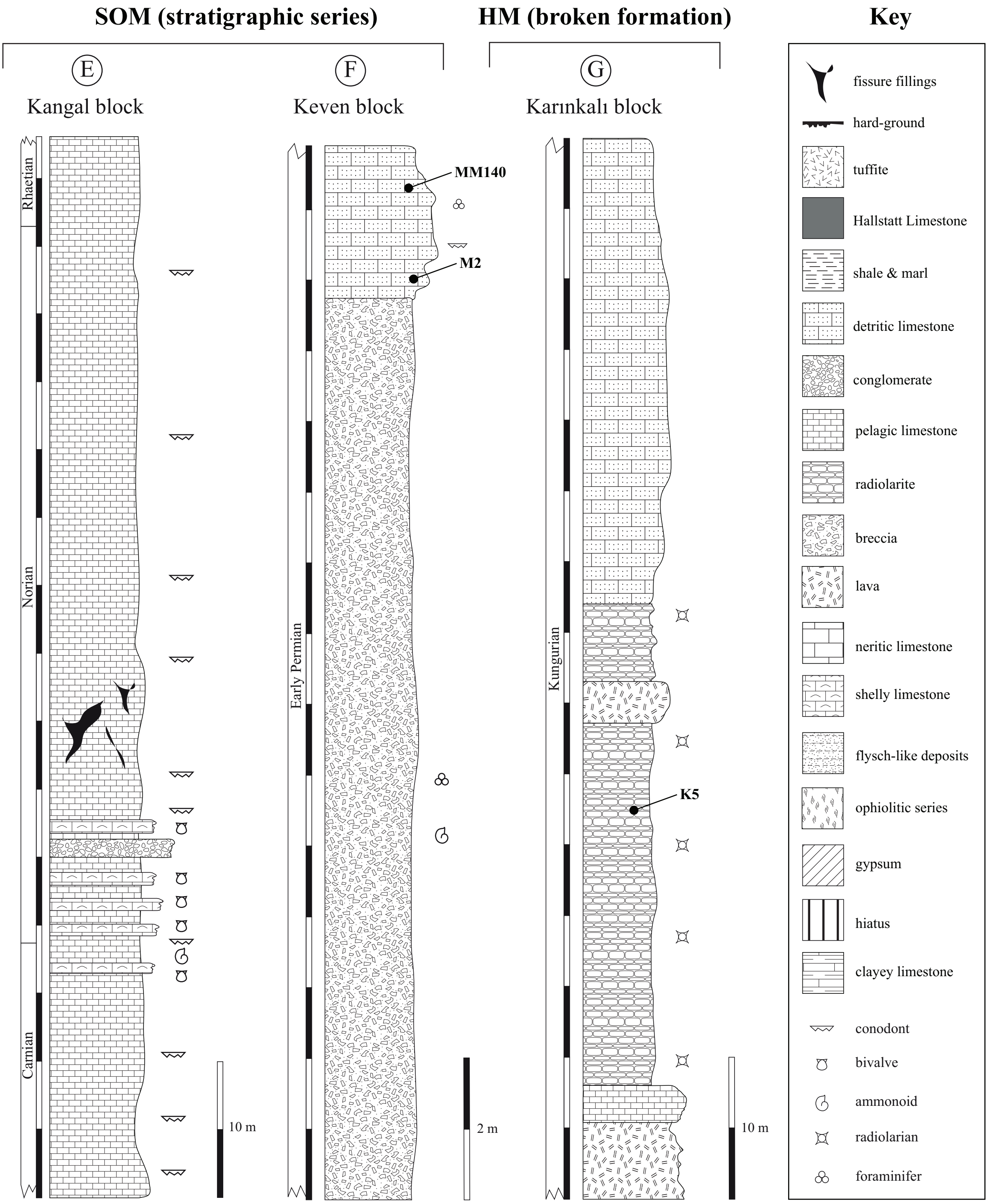

Figure 6. Synthetic lithostratigraphic sections of the broken formations and important stratigraphic sequences in the Sorgun and Hacialanı mélanges. Location of the logs on Figure 4.

facies locally rich in undetermined ammonoids, foraminifera and conodonts, and cut by neptunian dykes. *Halobia radiata* Gemmellaro, *H. styriaca* Mojsisovics, *H. austriaca* Mojsisovics and the ammonoids *Projuvavites* sp. are all characteristic of the Carnian–Norian boundary interval and are found in the middle part of the block. The conodonts from the Kangal block prove the presence of all Tuvalian zones of the early Norian up to the lower *E. triangularis - N. hallstattensis* Zone. The depositional environment of this formation could be either distal, or in a topographic high (plateau) swept by currents, or on the slope of an ocean or other deep water area far away from sediment-supplying marginal areas.

The Gerdemelipınarı block is about 10 m thick and is made of pink to red micritic limestones in the typical Hallstatt Limestone facies ranging from the middle Carnian to the late Norian. It is medium bedded at the base and thin bedded and very condensed at the top. The sequence comprises shelly limestones rich in *Halobia* spp. and in undetermined ammonoids. The Fırıntaş block is about 10 m thick and is embedded in a sheared serpentinous peridotite matrix. The section starts with middle Norian reddish and massive beds rich in ammonoids, continues with medium-bedded grey to pink micritic limestones and ends with earliest Rhaetian thin-bedded pink micritic and nodular limestones with primary cherts. All the section is in Hallstatt Limestone facies and the fauna is pelagic (ammonoids, conodonts, radiolaria, bivalves, fish remains and foraminifera). The Çardak block is characterized by 50 m of thin- to medium-bedded grey to pink micritic and nodular limestones, with ages ranging from middle to latest Norian. The fauna, including ammonoids, conodonts, radiolaria and foraminifera, is fully pelagic. The Zindan block is about 10 m thick and is enclosed by the ultramafic-type matrix. It comprises thin- to medium-bedded black nodular and fetid early to late Spathian micritic limestones containing conodonts and radiolaria. The environment is interpreted as pelagic.

The Keven block (Figures 4 & 6F, Table 1) is about 25 m thick and is embedded in the ultramafic-type matrix close to the boundary with the HM. This succession is represented by a polygenic yellowish breccia at the base interpreted as several mass-flow deposits. The clasts present an eclectic association of fossils from different environments characterized by ammonoids, crinoids, bryozoans, ostracods, brachiopods and fusulinids. One block yielded a Late Pennsylvanian–Early Permian assemblage composed of *Tubiphytes*? sp., *Eotuberitina reitlingerae* Miklukho-Maklay, *Endothyra* sp., *Globivalvulina bulloides* (Brady), *Climacammina* sp., *Calcitornella* sp. and *Schubertella* ex gr. *paramelonica* Suleimanov. Additionally, a large Sakmarian foraminifer *Zellia* cf. *nunosei* Hanzawa was found in another clast. The breccia is followed by two metres of bioclastic packstone presenting the A, B, C and D facies of the Bouma sequence. One sample (Sample M2, Table 1, Figure 6F) just above the breccia yielded *Tubiphytes* sp., *Epimastopora* sp., *Kamaena* sp. (Plate 4, Figure 7), *Eotuberitina reitlingerae* Miklukho-Maklay, *Tuberitina* sp. (Plate 4, Figure 6b), *Asselodiscus davydovi* Vachard & Moix, in review (nomen nudum) (Plate 4, Figure 1), *Lasiodiscus* sp., *Pseudovidalina modificata* (Potievskaya) (Plate 4, Figure 2), *Spireitlina*? sp. (Plate 4, Figure 4), *Climacammina* sp., *Deckerella* sp., *Tetrataxis* sp., *Globivalvulina vulgaris* Morozova (Plate 4, Figure 5), *Schubertella* ex gr. *paramelonica* Suleimanov (Plate 4, Figures 3b?, 6a), *Boultonia* sp. (Plate 4, Figure 3a), *Calcivertella* sp. and fragments of keriotheca of Schwagerinoidea. This assemblage is comparable with the Auernig Group of the Carnic Alps, i.e. dated as Orenburgian (= latest Pennsylvanian in age), but indicates the reworking of different Pennsylvanian levels. The shallow water conodont *Streptognathodus* cf. *rectangularis* Chernykh & Ritter, characteristic of the early Asselian, was also identified within this sample, thus indicating the youngest age of the sediment. Another sample (Sample MM140, Table 1, Figure 6F) from the upper part of the section yielded the cyanobacteria s.l. *Tubiphytes obscurus* Maslov and *Bacinella* sp., the algae *Permocalculus*? sp. and the foraminifera *Eotuberitina reitlingerae* Miklukho-Maklay, *Tuberitina bulbacea* Galloway & Harlton, *Tetrataxis conica* Ehrenberg, emend. Möller, *Climacammina* sp., *Schubertella* sp., *Calcitornella* sp., *Nodosinelloides* sp. and Schwagerinoidea (*Chusenella*? sp.). This assemblage shows that this part of the succession is probably late Early Permian in age (i.e. Artinskian–Kungurian).

The Hacialanı Mélange (HM)

The HM occupies the lowest tectonic position in the southern part of the investigated area (Figure 4), directly below the Mersin ophiolite. This peculiar position is probably due to tectonic complications during the Alpine tectonics. Tertiary sediments cover indifferently the ophiolite, the SOM and the HM. Compared to the SOM, well-developed broken formations are less common in the HM, and its components are genetically different. Most of the collected samples predate the Middle Triassic but a few younger blocks were found, notably two radiolarite samples indicating respectively Dogger (post-Aalenian, most probably Bajocian) and Valanginian ages, and a block of micro-breccia containing both fusulinids and fragments of rudists indicating a Late Cretaceous age. These younger blocks were obviously admixed during the final emplacement and juxtaposition of both mélanges (e.g., Norman 1993, Ankara region). They could also represent the younger sequence above the Triassic olistostrome in a distal position, compared to the more proximal Bolkardağ (Figure 2C).

Matrix and Blocks of the Hacialanı Mélange– The matrix of the HM may partly correspond to the Sorgun formation of Pampal (1987). It comprises argillites, silts, clays and sandstones and is well-exposed in the southern part of the investigated area (Figure 4). The Sorgun formation is described as a Maastrichtian–lower Palaeocene wildflysch containing Permian, Upper Triassic, Jurassic and Lower Cretaceous limestone blocks, with Cenomanian–Campanian radiolarite olistoliths. Palynological investigations in the matrix has shown that the material is mainly composed of land plant-derived bisaccates such as *Triadispora* sp. Klaus, *Striatoabieites aytugii* Visscher, *Lunatisporites pellucidus* (Goubin) Henelly, *Ovallipolis pseudoalatus* Thiergart, and *Endosporites papillatus* Jansonius. *O. pseudoalatus* ranges from late Anisian to Rhaetian, *S. aytugii* occurs in the Anisian to Ladinian, and *Triadispora* in the Middle and Late Triassic. *L. pellucidus* and *E. papillatus* are Early Triassic forms. There is no form which begins in the Carnian or later. This suggests a late Anisian to Ladinian age with some reworked Early Triassic sporomorphs in the matrix. Whereas a pre-late Anisian age can be excluded, a Late Triassic upper age can neither be proven nor excluded.

At places, a highly sheared greenish to mauve shaly matrix is clearly associated with brownish turbiditic sandstones with plant remains. The sporomorph association is composed of land plant-derived bisaccates like *Lunatisporites* sp. and *Platysaccus papilionis* Potonié & Klaus. These forms are obviously reworked, and so do not allow the dating of the matrix. Along the road from Sorgun to Poyrazlı, it is possible to follow about 400 m of argillites intercalated with micro-conglomerates, silts and sandstones with plants. The sandstones often show graded bedding with flute casts and bioturbations on the surface. The sporomorph association here is mainly composed of tricolpate pollens of Jurassic–Cretaceous age. In conclusion, it is possible to underscore the occurrence of two different generations of matrix in the HM: the earlier of Middle to Late Triassic age, when the HM was deposited as olistostromes in the Neotethys basin; the second during Jurassic–Cretaceous times (and most probably in the Late Cretaceous) when the two mélanges (SOM + HM) combined. In the southern part of the studied area near Kozan Deresi (a NE–SW-oriented valley west of Hacialanı, Figure 4), another type of matrix occurs, mainly composed of shale, debris-flows and turbiditic sandstones. Polymict debris-flow deposits present a large panel of different detrital facies. The latter were not investigated in detail but clasts are usually well-rounded and are mostly carbonates, sandstones, radiolarites, pebbles of quartz and rhyolites, tuffs, dolomites and lydites. The sandstones are often deformed and exhibit cm- to dm-size inclined north verging folds. Below the contact with the ophiolite, the matrix is made of a mixture of sandstones and radiolarites, and metre-scale blocks of neritic limestones rich in fusulinids. Here, we identified folded Ladinian radiolarian cherts, and two younger cherts of Late Jurassic and Early Cretaceous age embedded in the matrix (see below).

The dominating lithologies are Permian and Triassic radiolarites, Middle Triassic basalts, Early Permian slope sediments, plus Upper Triassic sandstones and conglomerates. The oldest identified rock is a block of violet grainstone showing an intense reworking of different Bashkirian, Moscovian, Kasimovian, Gzhelian and Early Permian faunas (Sample 355, Table 1, Figure 4). This block yielded a palaeogeographically very important late Asselian slope fauna. The age is given by *Streptognathodus barskovi* (Kozur), which occurs in both deep and shallow water facies, but not in very shallow water carbonate platform environments. It contains reworked late Gzhelian (Orenburgian) *Streptognathodus bellus* Chernykh & Ritter, which indicates the same environment as *S. barskovi*. Especially interesting is a rich reworked Kasimovian fauna containing *Idiognathodus toretzianus* Kozitskaya, *I. magnificus* Stauffer & Plummer, *Streptognathodus* cf. *elegantulus* Stauffer & Plummer, *Mesogondolella* n. sp. (= *Gondolella clarki* Koike in Einor 1979) and *Gondolella* n. sp. (= *Gondolella sublanceolata* Gunnell in Kozitskaya *et al*. 1978). Additionally, the Pennsylvanian *Idioprioniodus* sp. is present. *I. toretzianus*, *I. magnificus* and *Streptognathodus* cf. *elegantulus* occur in the same environment, as *S. barskovi*. *Gondolella* and *Mesogondolella* never occur in shallow water platform carbonates but only in deep water basinal or slope settings. *Idioprioniodus* sp. is a shallow water form which may also occur in slope sediments (transported from the shallow water). Because of its long range, it is not clear whether it belongs to the Kasimovian fauna. Without this species, the Kasimovian fauna would be a basinal deep water fauna; with this species, the fauna indicates a slope development between basinal deep water and shallow water deposits. Both environments have the same palaeogeographic meaning. In the Carboniferous, the Tauric platform had only a shallow water platform development, in which *Gondolella* and *Mesogondolella* did not occur. This grainstone contains also metazoan fragments such as bryozoans, brachiopods, crinoids, ostracods, the algae and pseudo-algae *Koivaella permiensis* Chuvashov, *Archaeolithoporella hidensis* Endô (Plate 4, Figure 15b), *Foliophycus*? sp., *Beresella* sp., *Dvinella comata* Khvorova (Plate 4, Figure 12a), *D.* sp., (Plate 4, Figures 12b, 17a), *Tubiphytes obscurus* Maslov (Plate 4, Figures 15a, 17b), *Ungdarella* sp. (Plate 4, Figure 16c), the foraminifera *Eotuberitina* sp., *Endothyra* sp., *Climacammina* sp., *Tuberitina bulbacea* Galloway & Harlton, *Globivalvulina mosquensis* Reitlinger, *G.* ex gr. *bulloides* (Brady), *Schubertella kingi exilis* Suleimanov (Plate 4, Figure 13), *S.* ex gr. *melonica* Dunbar & Skinner (Plate 4, Figure 14), *Schubertella* sp. (Plate 4, Figure 16b), *Protriticites* sp., and indet. Schwagerinoidea (Plate 4, Figure 16a). The fauna shows that this block cannot be derived from the Tauric platform. Pennsylvanian basinal and slope sediments are not known in the western Neotethys. Facies of this age occur only at the margin of the Palaeotethys or on the slope of seamounts within the Palaeotethyan realm as in the Tavas Nappe (Kozur *et al.* 1998; Vachard & Moix, in review) or in Iran (Bagheri & Stampfli 2008). Masset & Moix (2004) considered this block as belonging to the SOM. As stated above, the faunal content indicates derivation from the Palaeotethys. Thus, this outcrop may represent a tectonic window of the HM below the SOM, or it could have been admixed to the SOM during Late Cretaceous obduction.

Only a few shallow-water carbonates were accurately dated in the HM. These are mostly oncoid-bearing Early Permian limestones rich in fusulinids, crinoids, bryozoans, ostracods, echinoderm fragments and algae. One microrudstone (Sample 378, Table 1, Figure 4) with very rare fragments of volcanites (Plate 4, Figure 9a, b) and with crinoids yielded *Archaeolithoporella hidensis* Endô, *Tubiphytes* sp., *Eotuberitina* sp., *Reichelina* sp. (Plate 4, Figure 8), *Tuberitina* sp., *Globivalvulina vonderschmitti* Reichel, *Neoschwagerina* sp. and *Schubertella* cf. *silvestrii* Skinner & Wilde. The presence of *Neoschwagerina* sp. and *Reichelina* sp. (Plate 4, Figure 8) shows that the age is Capitanian. Another bioclastic packstone (Sample 325, Table 1, Figure 4) yielded *Tubiphytes* sp., *Tuberitina collosa* Reitlinger, *Neoendothyra* sp., *Tetrataxis* sp., *Lasiodiscus* sp., *Pachyphloia* sp., *Eotuberitina* sp., *Climacammina* sp., *Calcivertella* sp., *Calvezina ottomana* Sellier de Civrieux & Dessauvagie (Plate 4, Figure 11), *Globivalvulina vonderschmitti* Reichel, *Dunbarula schubertellaeformis* Sheng (Plate 4, Figure 10) and undetermined Neoschwagerinoidea (either reworked *Cancellina* or immature *Neoschwagerina*). The pelagic conodont *Mesogondolella intermedia* (Igo) marking the Kungurian was also found. The younger age is probably Capitanian, with the reworking of several Middle Permian shallow water and Early Permian pelagic faunas.

Other important samples are radiolarites, found either floating in the matrix or as elements in breccias or in broken formations. One Kungurian radiolarian chert (Sample 383, Table 1, Figure 4) yielded *Pseudoalbaillella scalprata* Holdsworth & Jones, *P. scalprata postscalprata* Ishiga and *Spinodeflandrella sinuata* (Ishiga & Watase). One Wordian radiolarian chert (Sample MM174, Table 1, Figure 4) yielded *Pseudoalbaillella eurasiatica* Kozur, Krainer & Mostler (Plate 3, Figures AA, AC), *Parafollicucullus fusiformis* Holdsworth & Jones (Plate 3, Figures AB, AE), *P. globosus* Ishiga & Imoto, *Pseudoalbaillella* sp., *Latentifistula* sp. and *Cauletella* cf. *manica* (De Wever & Caridroit) (Plate 3, Figure AD). This sample belongs to the upper part of the *P. globosus* - *P. fusiformis* Zone. Another late Wordian radiolarian chert (Sample 384, Table 1, Figure 4) yielded *Parafollicucullus globosus* Ishiga & Imoto, *P. fusiformis* Holdsworth & Jones, *Libella aurita* Rudenko, *Kimagior* sp. and *Quadriremis* sp. This sample belongs to the upper part of the Kungurian *Parafollicucullus globosus* Zone.

Locally, well-bedded dark green tuffites of supposed Artinskian/Kungurian age are conformably overlain by calciturbidites recycling green tuffites. They are in turn overlain by Kungurian radiolarites and Kungurian (?) calciturbidites. A radiolarian chert (Sample 329, Table 1, Figure 4) associated with green tuffites yielded *Pseudoalbaillella scalprata scalprata* Holdsworth & Jones, *P. scalprata postscalprata* Ishiga and several Ruzhencevispongacea. Another radiolarian chert of Guadalupian (probably Roadian) age (Sample MM173, Table 1, Figure 4) associated with limestones, greywackes and tuffs yielded an assemblage composed of *Pseudoalbaillella postscalprata* Ishiga (Plate 3, Figures J, K & L), *Quinqueremis* sp. (Plate 3, Figures M, N), ?*P. rhombothoracata* Ishiga & Imoto (Plate 3, Figure O), *Latentifistula* sp. (Plate 3, Figure P), *Gustefana*? sp. (Plate 3, Figure Q), *Ishigaum trifustis* De Wever & Caridroit (Plate 3, Figure R), *Spinodeflandrella*? sp. (Plate 3, Figures S, U & V), *S.* cf. *siciliensis* Kozur (Plate 3, Figures T, V), *S.* spec. indet. (Plate 3, Figure X), *Latentifistula* sp. (Plate 3, Figure Y) and Follicucullidae, gen. and sp. indet. (Plate 3, Figure Z).

The youngest pelagic sediment is a Valanginian radiolarian chert (Sample J2, Table 1, Figure 4) which yielded *Archaeodictyomitra* cf. *apiarium* (Rüst), *Dicerosaturnalis dicranacanthos* (Squinabol), *Emiluvia chica* Foreman, *Hemicryptocapsa* cf. *capita* Tan, *Pantanellium squinaboli* (Tan), *Praecaneta cosmoconica* (Foreman), and *Svinitzium depressum* (Baumgartner). The Dogger (post-Aalenian, most probably Bajocian) sample is a radiolarian chert (Sample MM157, Table 1, Figure 4) characterized by *Stichocapsa convexa* (Yao), *Triversus japonicus* Takemura, *Transhsuum* sp., and *Tricolocapsa*? spp. As stated above, these two samples are found immediately below the ophiolite in the southern part of the investigated area (see Figure 4). Lower Cretaceous radiolarian cherts were also identified in the SOM (see above). Thus, a direct derivation from the Mersin ophiolite should be envisaged.

Broken Formations of the Hacialanı Mélange– The Karinkalı block (Figures 4 & 6G, Table 1) is a 150-m-thick sequence embedded in the argillite and sandstone-rich matrix. The lateral extent of this broken formation is relatively moderate (hundreds of metres), and its lithological components are sometimes reproduced at lower-scale elsewhere in the HM, especially in the upper part of the sequence which is made of characteristic calciturbidites (calcarenites reworking green tuffites and yellow dolomites, plus quartz, micas and feldspars). The sequence starts with a sill (8 m) of lamprophyre, followed by 2 m of medium-bedded highly recrystallized pelagic limestones. It passes up into 25 m of argillaceous Kungurian radiolarites, which are overlain by a 3 m lamprophyre sill. The top of this formation consists of 6 m of argillaceous Kungurian radiolarites, followed by thick calciturbiditic deposits. In the middle part of the section, the radiolarian assemblage (Sample K5, Table 1, Figure 6G) includes *Pseudoalbaillella scalprata scalprata* Holdsworth & Jones, *P. scalprata postscalprata* Ishiga, *Foremanconus* sp., *Latentifistula* sp., *Spinodeflandrella siciliensis* Kozur, and *S.* sp.

South of Sorgun, the sedimentary matrix is nearly absent, and sharp contacts between blocks or slices of different lithologies can be observed. Along the Sorgun River, three different mappable and coherent units have been identified. They are from south to north: (1) a hundred-metre-thick broken formation composed of Kungurian radiolarites followed by calciturbidites (Karinkalı block); (2) a broken formation with pillow lavas at the base followed by a radiolaritic sequence in stratigraphic contact. The basalts show E-MORB or arc-related geochemical signatures, whereas the sediments between the pillow lavas indicate a latest Anisian age. The lowest radiolarian assemblage (Sample J9a, Table 1) is characteristic of the late Illyrian *Kellnerites felsoeoersensisis* Zone and includes *Pseudoertlispongus angulatus* Kozur, *Paroertlispongus multispinosus* Kozur & Mostler, *Triassocampe* sp., *Pseudosylosphaera* sp. and *Eptingium nakasekoi* Kozur & Mostler. The uppermost radiolarian assemblage (Sample J9b, Table 1) belongs to the latest Illyrian *Reitzites reitzi* Zone and contains *Oertlispongus inaequispinosus* Dumitrică, Kozur & Mostler, *O. primitivus* Kozur & Mostler, transitional to *Pseudoertlispongus*, *Pseudoertlispongus mostleri* Kozur, *P.* sp., *Triassocampe scalaris* Dumitrică, Kozur & Mostler and *Pseudostylosphaera coccostyla* (Rüst), *P.* sp., *Eptingium* sp., *Paroertlispongus* sp., *Paurinella* sp., *Vinassaspongus* sp., *Hozmadia* sp. and *Falcispongus falciformis* Dumitrică; (3) another hundred-metre-thick broken formation made of thin-bedded and highly folded black micritic limestones yielded (Sample 129/06, Table 1) conodonts of Spathian age including the index species *Neospathodus homeri* (Bender).

Regional Correlations and Discussion

This section aims (1) to discuss the correlations of the Sorgun and Hacialanı mélanges with data from the regional geology (Figure 7) and (2) to examine their consequences in term of palaeotectonic and palaeogeographic evolution (Figure 8), focusing successively on the correlations of the platform, slope and basin units. It is obvious that some units of the Mersin mélanges could be compared with the Beyşehir-Hoyran, Antalya and Lycian nappes, and with Baër-Bassit and Mamonia (e.g., Parlak & Robertson 2004). Below, we present further evidence of these correlations, comparing elements of the Mersin mélanges (from single facies to coherent stratigraphic sequences) to those of the Anatolian terrane (i.e. the Beyşehir-Hoyran and the Lycian nappes, the Bozkır-Karaman-Ermenek units) on one hand, and to the South Taurides Exotic Units (i.e. the Antalya Nappes, Mamonia) on the other hand (see Moix *et al.* 2008a). Additional correlations with other localities of the Tethyan realm (e.g., Greece, Italy, and Iran) will also be proposed.

Platform Units

In the Mersin mélanges, the main lithologies are recrystallized platform-type carbonates (Figure 9). Between Güzeloluk and Sorgun, the Carboniferous–Lower Cretaceous Göktepe Limestone was mapped as a thrust sheet overriding the Mersin mélange (Pampal 1987; Parlak 1996). The Göktepe Limestone may be correlated with the Jurassic–Cenomanian Cehennemdere formation in the Arslanköy area (Demirtaşlı *et al.* 1984; Özer *et al.* 2004) and with the Jurassic–Late Cretaceous Çağıloluktepe Limestone in the Arslanköy-Tepeköy area (Pampal 1984). Finally, the Göktepe Limestone, the Cehennemdere formation and the Çağıloluktepe Limestone are comparable, and most probably belong to the Bolkardağ paraautochthon. Between Gâvuruçtuğu and Sorgun in the SOM (Figure 4), Parlak & Robertson (2004) reconstructed an intact Late Permian to Early Cretaceous shallow-water platform derived from the Bolkardağ and incorporated into the ophiolitic mélange.

New palaeontological and tectonostratigraphic evidence presented above demonstrate the exotic nature of some of the platform carbonate blocks. This is so for the Talvarlıyurt block (Figure 5A), composed of Upper Triassic to Lower Jurassic neritic limestones at its base. The Jurassic to Cretaceous pelagic sedimentation, together with the deposition of a wildflysch above Cenomanian radiolarites indicate an early flexuration of a margin typical of the Anatolian domain (Moix *et al.* 2008a). Also, the post-Anisian and pre-latest middle Carnian age for the shallow-water limestones at the base of the Tavusçayırı block, together with the presence of the Huğlu-type tuffites and the development of the

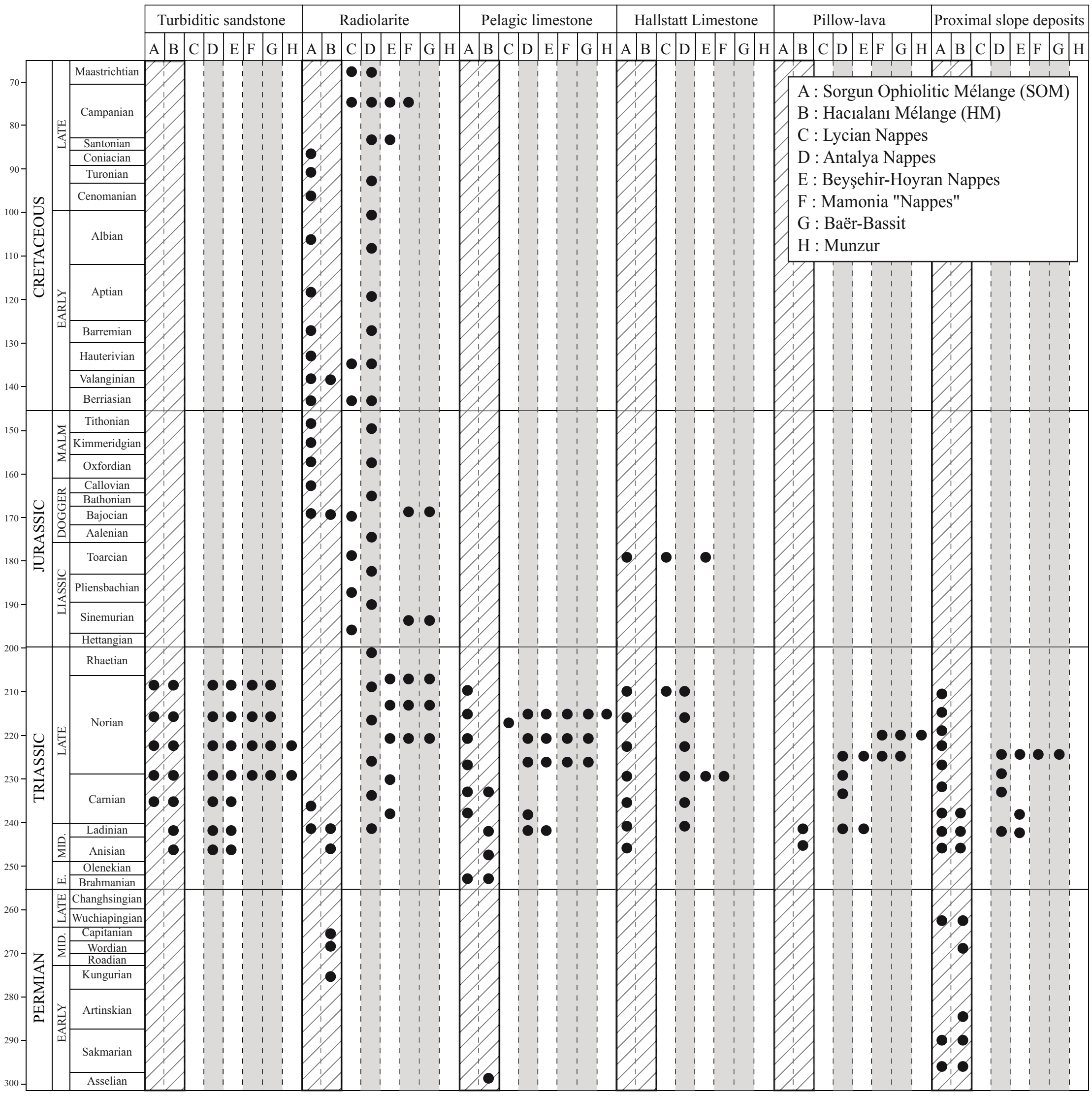

Figure 7. Synthetic facies comparison for different nappe systems in Turkey, Cyprus and Syria, compiled from Ricou *et al.* (1984), except for the Sorgun and Hacialanı mélanges. Columns in grey are located north of the Bolkardağ whereas the others are south of it. The hatched ones relate to the Mersin mélanges. Same geological time scale as Figure 2.

Upper Triassic pelagic limestones above them, indicate rifting in Middle–Late Triassic times. Thus, an Anatolian terrane northern margin origin is indicated for this series. Further clues come from the Gâvuruçtuğu and Kocatabur blocks. The Gâvuruçtuğu block at its base is composed of a middle Norian ramp-type marl-limestone alternation, followed by late Norian, Rhaetian and probably Lower Jurassic shallow water limestones. The presence of the middle Norian *Epigondolella praeslovakensis* conodont fauna suggests a Neotethyan origin for this block (Moix *et al.* 2007b). The Kocatabur block is composed of a post-latest Carnian to pre-latest Rhaetian neritic series overlying late Carnian pelagic limestones. The latest Carnian fauna with *Metapolygnathus mersinensis* and common *Metapolygnathus primitius sensu stricto*, indicate a Neotethyan origin also (Moix *et al.* 2007b).

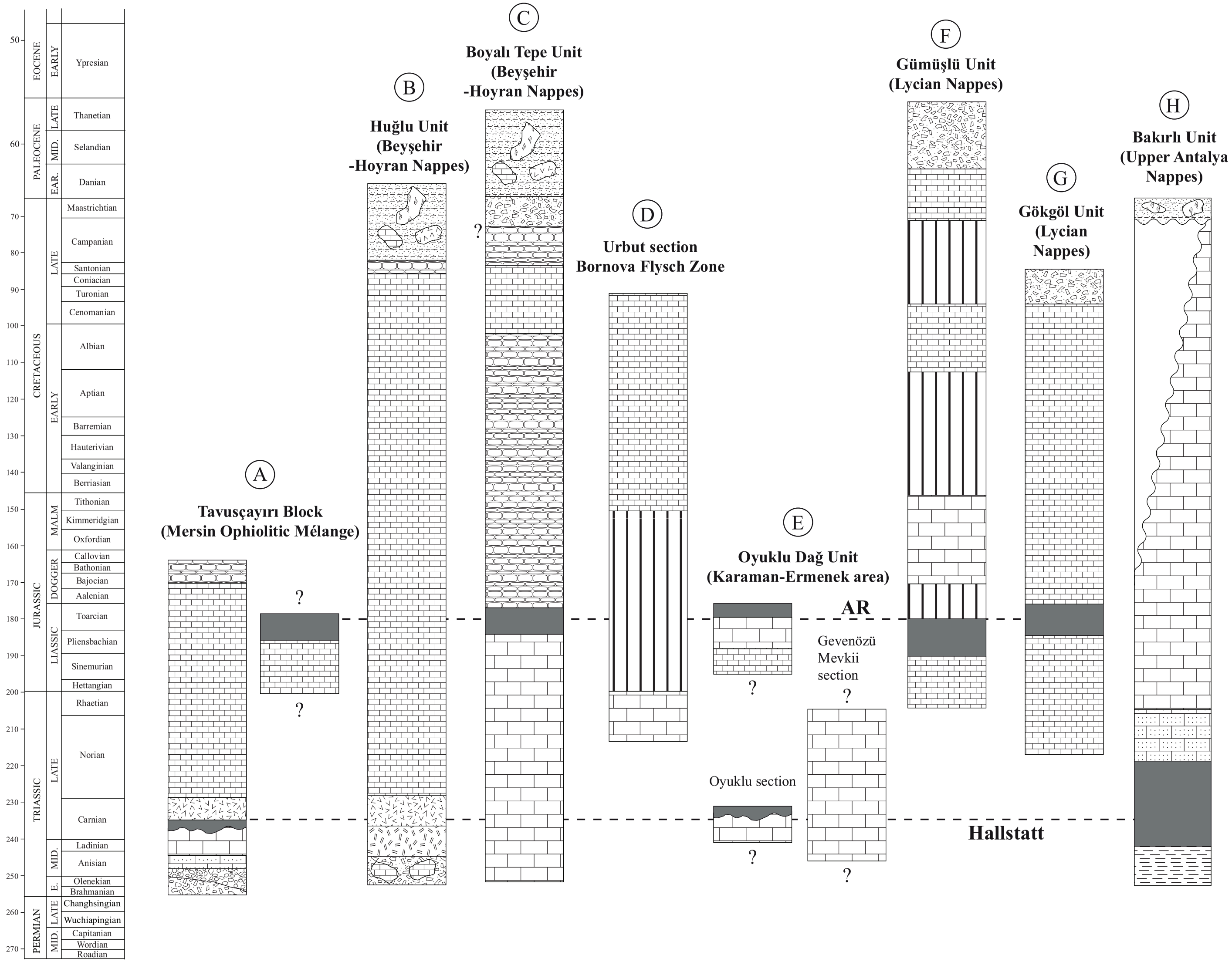

Figure 8. Correlations between broken formations in the Mersin mélanges and similar sequences in the Hadım, Beyşehir-Hoyran, Lycian and Antalya Nappes. **(A)** this work; **(B)** compiled from Gökdeniz (1981), Monod (1977) and Özgül (1984); **(C)** modified from Monod (1977); **(D)** modified from Okay & Altıner (2007); **(E)** modified from Gökdeniz (1981); **(F)** compiled from Poisson (1977) and Gutnic *et al.* (1979); **(G)** modified from Gutnic *et al.* (1979); **(H)** modified from Marcoux (1987). Same geological time scale as Figure 2 and key on Figure 6.

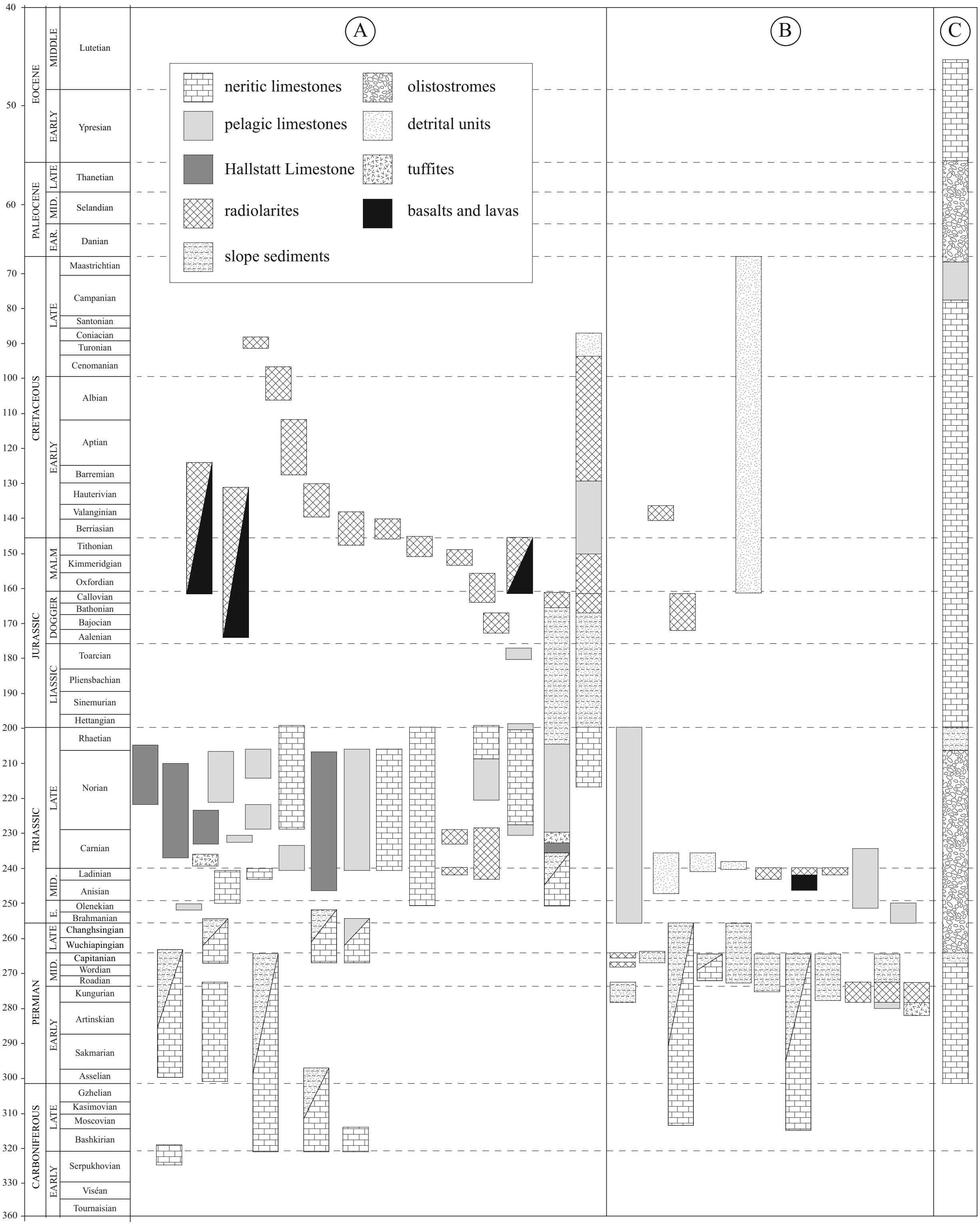

Figure 9. Summary table of the ages and facies found in the Mersin mélanges. **(A)** Sorgun ophiolitic mélange; (B) Hacialanı mélange; (C) Bolkardağ parautochthonous. Same geological time scale as Figure 2.

In conclusion, some neritic sequences found in the mélanges are exotic and are derived either from the Anatolian terrane or from the Neotethyan domain. There is no direct evidence of a continuous platform from the Permian to the Cretaceous, as stated by Parlak & Robertson (2004). However, it cannot be excluded that some isolated blocks could have been detached from the paraautochthonous unit during obduction and admixed to the Upper Cretaceous Sorgun mélange.

Slope Units

Tuffitic Units– Green tuffites with an alkaline geochemical signature (WPB-type) sometimes associated with Kungurian radiolarites and turbidites are found exclusively in the HM (Figure 9). Similar Kungurian sequences are known from Palaeotethys series in NE Iran, where the volcanics either underlie seamounts or are interstratified in pelagic rocks at the slope and base of seamounts (Kozur & Mostler 1991; Bagheri *et al.* 2003; Bagheri & Stampfli 2008). Upper Triassic tuffites are well-exposed in the SOM and correspond to the Huğlu volcanism. The tuffitic development of the Tavusçayırı block can be compared to typical Anatolian series, such as in the Beyşehir-Hoyran Nappes (Monod 1977; Gutnic *et al.* 1979; Parlak & Robertson 2004), in the Oyuklu Dağ unit near Ermenek (Gökdeniz 1981), and in the Bozkır units (Özgül 1976, 1997).

Before our study, the age of this regional tuffitic episode was poorly known. At the type locality in Huğlu, a minimal Anisian–Ladinian age was indicated by shallow-water fossils reworked in volcanic breccias (Monod 1977; Gökdeniz 1981; Özgül 1997). Radiolarian assemblages obtained from limestones intercalations at the base of the Huğlu tuffites indicate a middle Carnian age (Kozur 1997; Tekin 1999; Tekin *et al.* 2001). In the Tavusçayırı block, the tuffs conformably overlie well dated late middle Carnian Hallstatt Limestone (Figure 5B). In the Oyuklu Dağ unit, massive reef limestones are also filled by late Carnian Hallstatt Limestone (Gökdeniz 1981). By analogy with Mersin, these limestones overlain by Hallstatt limestone could be seen as the substratum of the Huğlu tuffites. The Huğlu tuffites are sometimes associated with brownish altered lavas and tuffs. Interstratified limestones at their base yielded a middle Carnian ammonoid, consistent with the ages found in the Tavusçayırı block. Lower to middle Upper Carnian Huğlu-type tuffites associated with sandstones and nodular limestones were recently identified near Elbistan (Tekin & Bedi 2007a, b).

In the Tavusçayırı block, the end of the tuffitic development is marked by the deposition of the Huğlu Limestone indicating a latest Tuvalian or an earliest Norian age. At the type locality in Huğlu, the tuffites are conformably overlain by the Huğlu Limestone formerly assumed to be Middle Triassic at their base and Cenomanian–Campanian at their top (Monod 1977; Gutnic *et al.* 1979). Kozur (1997) considered that the Huğlu-type limestones begin in the upper Carnian and range up to the uppermost Triassic. In the Bozkır units, calcareous sedimentation above the tuffites began during the Late Triassic and persisted until the Santonian (Özgül 1997). In Elbistan, the tuffs are overlain by late Carnian to Norian pelagic limestones (Tekin & Bedi 2007a, b). In the Oyuklu Dağ unit, a middle–late Norian age is assigned to the Huğlu Limestone, which overlies Carnian green tuffites (Gökdeniz 1981; Gallet *et al.* 2007).

In conclusion, the Huğlu development in the SOM shows an indisputable stratigraphic continuity between part of the Oyuklu Dağ unit and part of the Huğlu unit in its type locality. Typical Pindos sequences found in the Peloponnese, in Crete and in the Dodecanese islands present the same type of series (Degnan & Robertson 1998; Stampfli *et al.* 2003; Moix *et al.* 2008b; Moix & Stampfli 2009; Moix 2010). The deposition of Hallstatt limestone above shallow-water limestones during the middle Carnian corresponds to the Huğlu-Pindos signal (Stampfli & Kozur 2006; Moix & Stampfli 2009). This signal is also identified in typical Pindos sections in the Peloponnese, where upper Cordevolian pelagic limestones associated with lavas were recognized (Tsoflias 1969; Degnan & Robertson 1998). The Huğlu-type sequences are related to the latest extensional events leading to back-arc openings in the Variscan cordillera in the Late Triassic (i.e. opening of the Huğlu-Pindos Ocean). These events are marked by widespread volcanism and led finally to the onset of a passive margin setting that lasted until the Late Cretaceous obduction of supra-subduction type ophiolites over the north Anatolian margin.

Breccias, Sandstones and Conglomerates– Carboniferous, Early to Late Permian and Triassic (until the Norian) proximal slope and distal gravity-flow deposits are found in the Mersin mélanges (Figures 7 & 9). We interpret the Pennsylvanian and the Lower Permian slope facies as most probably derived from the Palaeotethys. As said above, Pennsylvanian and pre-Kungurian–Lower Permian slope deposits are not known from the western Neotethys, whereas Middle and Upper Permian slope sediments could have been derived from either the Palaeotethys or the Neotethys. In the HM, deep-water sediments are represented by Middle–Upper Triassic turbiditic clays and sandstones with plant remains, and showing abundant flute-casts. Locally, the identification of *Torlessia* spp. indicates Carnian or Norian ages for the deposits. These terrigenous sediments could be the matrix for the HM and are analogous to the late Anisian to lower Carnian Sicilian 'Lercara formation' with comparable palynomorph assemblages (Carcione 2007). Molasse-type greenish sandstones and conglomerates reworking quartz, rhyolite and lydite pebbles are often associated with the turbiditic sandstones. These molasse deposits are interpreted to be the product of the Late Triassic collision between the Anatolian and Taurus terranes (Cimmerian molasse, Moix *et al.* 2008a). In the SOM, turbiditic sandstones are rare and only found as small and scarce isolated blocks.

The Upper Triassic turbiditic sandstones with plants associated with *Halobia*-bearing pelagic limestones are common in the Antalya Nappes and are also found in Cyprus, Baër-Bassit (Syria) and in the Pindos sequences of Crete, Karpathos, Rhodes and Tilos. At the base of the upper Antalya Nappes, pelagic limestones interstratified in the sandstones yielded late Carnian conodonts (Hungerbühler *et al.* 2008). Sandstones with plant debris are identified in the Beyşehir-Hoyran Nappes (Gökdeniz 1981), and are found below the Huğlu-type tuffites. We regard these sandstones as potential syn-rift deposits of the Huğlu-Pindos Ocean. In eastern Turkey, the base of the Andırın Massif is characterized by Carnian–Norian greenish sandstones with plant remains, rhizomorphs and coal seams, interspersed by *Halobia*-bearing limestones (Pampal & Kurtman 1984). The easternmost locality of these Upper Triassic sandstones with plant remains are described in Baër-Bassit (Lapierre 1975; Delaune-Mayère *et al.* 1977). In the Mamonia 'Nappes' in Cyprus, the Vlambouros Formation (Lapierre 1975) comprises sandstones with plants intercalated by early to upper Norian *Halobia*-bearing limestones containing the conodonts *Epigondolella quadrata* Orchard, *Neohindeodella* sp., *E. postera* Kozur & Mostler, *Norigondolella steinbergensis* (Mosher), and *Mockina bidentata* (Mosher). Lapierre (1975) thought that these detrital units starting in the Norian persisted into the Jurassic (most probably limited to the Liassic). Similar sandstones are found at the base of Pindos-type sequences in Greece (Degnan & Robertson 1998; Stampfli *et al.* 2003; Moix *et al.* 2008b; Moix & Stampfli 2009).

Turbiditic sandstones often associated with molasse deposits were also present at the northern margin of the East Mediterranean/Neotethys (southern margin of the Taurus terrane) and are related to the closure of the Palaeotethys between the Taurus and the Anatolian terranes. Near Seydişehir, the Sarpiar Dere flysch-like sequence (Monod 1977) is interpreted to have been deposited in a middle Carnian to Norian piggy-back basin in front of the Cimmerian orogenic front. The Sarpiar Dere sandstones are coeval with the Carnian/Norian Kaşımlar formation (Gutnic *et al.* 1979), the latter being deposited in a flexural basin. In the Lycian Nappes, the Carnian–Norian Belenkavak formation of the Karadağ unit comprises sandstones, siltstones and shales including blocks of Permian limestones (Kozur *et al.* 1998; Vachard & Moix, in review), and probably represents an equivalent of the Sarpiar Dere formation. Some of the molasse deposits are represented by the widespread Upper Triassic–lower Liassic Çayır formation which is composed of red continental silts and sandstones, and conglomerates (Gutnic *et al.* 1979). This type of conglomerate has been also identified in the HM, in the Aladağ unit and in the Antalya Nappes (Moix & Stampfli 2009;

Martini *et al.* 2009; Moix *et al.* 2008b; Vachard & Moix, in review).

Upper Permian and principally Triassic detrital units constitute a major element in comparisons and play an important role in deciphering the geodynamic evolution of the Tethysides. In particular, the Late Triassic–Early Jurassic time interval sheds light on two different but quasi-synchronous geodynamic events. Some of the clastic units are related to diffuse rifting along the southern margin of Eurasia (e.g., Huğlu-Pindos rift sequences), whereas others reflect the Cimmerian collision between Gondwana and post-Variscan Eurasia-derived terranes (Moix *et al.* 2008b; Moix & Stampfli 2009). Because of the concomitant closure of the Palaeotethys and opening of the Huğlu-Pindos back-arc in the Palaeotethyan active margin, the source for the Upper Triassic clastics is difficult to establish. Only the evolution of the tectonostratigraphic units can bring enough constraints to replace these series in a coherent geodynamic scheme. In the Huğlu-Pindos Ocean, Carnian to Norian clastics (sometimes associated with lavas) interspersed with *Halobia*-bearing pelagic limestones are syn-rift sediments and are followed by a continuous pelagic sequence until the Palaeocene. On the Taurus terrane, Norian to Liassic platforms overlie the Cimmerian molasse deposits. In this case, the shallow marine sedimentation persists until the flexuration of the composite Anatolian-Tauric platform in Campanian–Maastrichtian times (e.g., Stampfli *et al.* 2003; Moix *et al.* 2008a).

The closure of the Palaeotethys in Late Triassic times between two crustally attenuated terranes caused minor inversions and locally the sedimentation continued with little disturbance. In other places, the Eo-Cimmerian relief was only transgressed in the Middle Jurassic (Monod 1977). After the Cimmerian event, the Anatolian and Taurus terranes formed a single entity, covered by large carbonate platforms of Jurassic age. The lower plate position of the Taurus terrane during the Eo-Cimmerian collision induced the development of foreland and piggy-back basins, filled-up with flysch and/or molasse deposits (e.g., Sarpiar Dere and Kaşımlar formations). We think that locally such flysch-like deposits overstepped the Cimmerian block and were deposited in the East-Mediterranean basin (Moix *et al.* 2008a). The Lower–Middle Triassic Gerdekesyayla formation in the northern Bolkardağ unit and the Lower–Middle Triassic Karagedik formation in the southern Bolkardağ unit (Figure 2A–C) are also marked by a large detrital input including reworked blocks of Permian age (Demirtaşlı *et al.* 1984). These Triassic detrital units are most probably a lateral equivalent of the HM. A similar type of reworking exists in Sicily, where it is clearly part of the Neotethys pelagic sequence (Stampfli *et al.* 2001). These deep-sea fans interstratified in the Neotethys sequence, were re-mobilized during the final emplacement of the Mersin-type or peri-Arabian ophiolites.

Basin Units

Basin Units in the Sorgun Ophiolitic Mélange– Both the Upper Triassic Hallstatt Limestone and Lower Jurassic Ammonitico Rosso Limestone are exclusively found in the SOM (Figures 8 & 9). Upper Triassic to Cretaceous basinal sequences are also a characteristic of the SOM, and these series could belong either to the Neotethys or to the Huğlu-Pindos Ocean. The Kangal, Gerdemelipınarı, Fırıntaş and Çardak blocks represent different stages of the same pelagic sedimentation in Hallstatt limestone facies ranging from the middle Carnian to the early Rhaetian. Contrary to other sequences described in Turkey and with the exception of the northern margin of the Küre Ocean which presents large amounts of Anisian to upper Norian or lower Rhaetian Hallstatt limestone (Kozur *et al.* 2000), the Triassic Hallstatt Limestone facies are well represented: they began in the Anisian and persisted until the late Norian. This type of Hallstatt Limestone facies is found as blocks of different sizes and presents many similar characteristics to the upper Antalya Nappes (Figures 7, 8 & 9). The similarities between the Kangal block and the Bölücektası and Kavaalanı sections from the Bakırlı Dağ unit are obvious (Marcoux *et al.* 1986).

In the SOM, the Toarcian Ammonitico Rosso Limestone is compared to well-known successions found in allochthonous sequences in Turkey (Figures 7, 8 & 9). The Boyalı Tepe and the Oyuklu Dağ units in the Beyşehir-Hoyran Nappes (Gutnic & Monod

1970; Özgül 1976; Gökdeniz 1981), the Gökgöl unit near Dinar (Gutnic *et al.* 1979), the Gümüşlü and the Domuz Dağ units in the Lycian Nappes (Brönnimann *et al.* 1970; Poisson 1977; Gutnic *et al.* 1979; Dommergues *et al.* 2005), and the Urbut section in the Bornova flysch zone (Okay & Altıner 2007) present a moderate to well-developed Ammonitico Rosso Limestone of comparable age. The Toarcian Ammonitico Rosso limestone of the SOM belongs to the Huğlu-type sequence and can be therefore best correlated to the Oyuklu Dağ unit in the Beyşehir-Hoyran Nappes. There, the Ammonitico Rosso limestone is followed by upper Pliensbachian to lower Toarcian cherty limestones, overlain by Aalenian to lower Bajocian radiolarian cherts. In the SOM, the radiolarian cherts are late Bajocian in age. The condensed units of Liassic age in southern Turkey suggest a common origin for these nappes, along the northern passive margin of the Anatolian terrane. The Liassic condensed level marks a starvation stage, followed by the generalized thermal subsidence of the margin.

Basin Units in the Hacialanı Mélange– The Middle to Upper Triassic matrix, the Pennsylvanian to Lower Permian pelagic and slope deposits, the Lower/Middle Permian and Middle Triassic radiolarites are exclusively found in the HM (Figure 9) and are probably derived from the Palaeotethys because these lithologies and facies are absent from Neotethyan sequences of this age (Moix *et al.* 2007a). Radiolarites of Kungurian age are unknown from the western Neotethys, where the oldest radiolarites have a (late) Wordian age. Kungurian radiolarites and pelagic limestones laid on tuffs and volcanics are common in the Palaeotethys of Iran (Kozur & Mostler 1991; Bagheri *et al.* 2003, 2004), where they are related to Early Permian seamounts within the Palaeotethys. The Middle Permian radiolarites could be derived from either the Palaeotethys or from the Neotethys, e.g., Sang-e-Sefid in the Palaeotethys of NE Iran or in the Neotethys of Oman.

Permian pelagic faunas are found in the Neotethyan realm of Sicily (Kozur 1990; Catalano *et al.* 1991, 1992; Kozur 1995). The opening of the Neotethys Ocean gave birth to a new passive margin along the northern side of Gondwana from Sicily to Timor, passing through the East Mediterranean basin, Oman and the Himalayas. The oldest fauna in the western Sicanian Basin is a latest Artinskian–Kungurian basinal microfauna that shows Pacific affinities. Middle Permian Hallstatt Limestone similar to that found associated to MORB in Oman (Niko *et al.* 1996) was also reported from the Sosio Complex by Kozur (1995). Its Guadalupian pelagic macro-fauna presents strong affinities with northern Iraq, Oman, Malaysia and Timor (Gerth 1950; Vašíček & Kullmann 1988; Blendinger *et al.* 1992; Sone *et al.* 2001). The Late Permian Albaillellaria fauna from red deep-sea clay in the Sicanian domain leads to the same conclusion (Kozur 1993). These facts imply a Middle–Late Permian direct deep water connection of the East-Mediterranean basin with the Neotethys. We consider the Middle–Late Permian Sicanian Basin to represent the northwestern end of the East-Mediterranean rift/ocean system. Late Artinskian and mainly Kungurian sediments/microfossils from the Palaeotethyan accretionary prism were recycled as olistoliths in the Neotethyan Roadian olistostrome unit, partly also in (?) Middle Triassic to middle Carnian siliciclastic turbidites and marls, or were later mixed with Upper Triassic limestones in a Tertiary tectonic mélange.

Carboniferous and Permian radiolarian cherts and other pelagic sediments were recognized in the Çal and Hodul units of the Karakaya Complex (Okay & Mostler 1994; Göncüoğlu *et al.* 2004), in the Tavas Nappe (Kozur *et al.* 1998; Moix *et al.* 2007c; Moix 2010; Vachard & Moix, in review), in the Çataloturan Nappe of the Bolkardağ unit (Göncüoğlu *et al.* 2007) and in the Baltalimani formation of the İstanbul block (Noble *et al.* 2008). In the Mersin mélanges, the Palaeozoic remnants found so far are Mississippian to Capitanian shallow marine and pelagic rocks. Among them, Early Carboniferous to Middle Permian shallow-water environments are not discriminating in terms of palaeogeography, as shallow water sedimentation of that age is well-developed both in the Anatolian and Tauric terranes. In contrast, Mississippian to Lower Permian pelagic and slope deposits, as well as Kungurian radiolarites clearly indicate a Palaeotethyan origin for parts of the HM.

One outcrop exhibits uppermost Anisian radiolarian cherts associated with WPB-type pillow lavas which show an arc tholeiitic affinity. Late Illyrian pillow lavas have never been described elsewhere in Turkey. The latest Anisian age excludes an Anatolian rift origin because the Huğlu-Pindos Ocean did not open till Late Triassic times. As the HM contains numerous evidence for Palaeotethyan remnants, these upper Anisian pelagic sediments can be seen as Palaeotethyan relics or as an eastern continuation of the Karakaya fore-arc basin, in which Anisian pelagic sediments are very common.

Conclusion

Extensive field work and numerous micropalaeontological determinations in the infra-ophiolitic mélanges of the Mersin ophiolite lead us to clearly differentiate two mélanges: the Upper Cretaceous Sorgun ophiolitic mélange and the Ladinian–Carnian Hacialanı mélange. We show that these mélanges display the mixed origin of different blocks and broken formations, as summarized below.

(1) The Palaeotethyan remnants are common and found exclusively in the Hacialanı mélange as small blocks and a few broken formations. Pennsylvanian and Lower Permian slope and basin deposits (calcarenites, radiolarites) are unknown from the western Neotethys but have been described in Palaeotethyan series in the Lycian Nappes and in the margins of displaced terranes in Iran. Radiolarites of Kungurian age are sometimes associated with abundant tuffites and are also unknown in the western Neotethyan realm, where the oldest radiolarites have a (late) Wordian age. Kungurian radiolarites and pelagic limestones overlying tuffs and volcanics are common in the Palaeotethys of Iran, where they are related to Early Permian seamounts within the Palaeotethys. These Palaeotethyan remnants within the HM were most likely reworked as major olistostromes in the Neotethys basin during the Eo-Cimmerian orogenic event.

(2) Neotethyan elements are represented by potential Middle–Late Triassic seamounts and by broken formations containing Neotethyan faunas. The abundance of *Metapolygnathus mersinensis* Kozur & Moix and *M. primitius sensu stricto* in the latest Carnian of the Kocatabur block, as well as the rich occurrence of the middle Norian *Epigondolella praeslovakensis* Kozur, Masset & Moix in the Gâvuruçtuğu block indicate a derivation from the Neotethys, but further studies in the latest Carnian to middle Norian interval of the Pindos, Antalya and Huğlu units are necessary to exclude the common occurrence of these two species in the Huğlu-Pindos Ocean, also exposed in the Antalya Nappes.

(3) The main Anatolian elements (upper plate position) are symbolized by sequences belonging to the northern passive margin of the Anatolian terrane (southern margin of the Huğlu-Pindos Ocean), outlined by the Late Triassic syn-rift volcanic event (Huğlu-type series also found in the Beyşehir-Hoyran Nappes), the early flexuration of the margin (already during the Cenomanian) and the Late Cretaceous obducted ophiolitic sequences. This margin is interpreted as emerging from the collapse of the former Variscan cordillera and opening of major back-arc type basins along the northern active margin of Palaeotethys during the Triassic.

(4) The Tauric elements (lower plate position) are represented by Eo-Cimmerian flysch-like and molasse sequences, intercalated in Neotethyan series starting most probably with pelagic Permian sediments totally absent from the Anatolian domain. Other blocks are most probably derived from the paraautochthonous sequences belonging to the Taurus-Beydağları marginal sequences.

The Mersin Ophiolitic Complex belongs to the South-Taurides Exotic Units, extending from Mersin to Antalya, and which can be widened to include the Mamonia ‘Nappes’ in Cyprus. This domain is made of exotic elements of the Anatolian terrane now found south of the Taurus terrane, juxtaposed with elements derived from the Palaeotethys/Neotethys/Taurus terrane, and emplaced onto the Taurus southern margin (Mersin) or Beydağları domain (Antalya) in Late Cretaceous–Palaeocene times (Moix *et al.* 2008a). In terms of palaeotectonic and palaeogeography, a direct implication is the need for (roughly E–W) lateral displacements of hundreds of kilometres to explain the present day structural scheme. In conclusion, the ages and distribution of the basin, slope and platform facies found in the mélanges, their faunal content, the age of the passive margin onto which the ophiolites were obducted, and the evolution of the stratigraphic series demonstrate that several Tethyan oceanic basins were involved in the formation of the southern Tauric ophiolitic nappes. The coexistence south of the Bolkardağ of these cosmopolitan units is of crucial importance in deciphering the regional palaeogeographic and palaeotectonic evolution.

Acknowledgements

The authors are very grateful to all our colleagues who participate in the study of various fossil groups. Their palaeontological expertise was a key point in the elaboration of this manuscript. We want particularly to express our gratitude to L. Carcione, M. Caron, S. Goričan, G. Gorin, J. Guex, L. Hottinger, C. Jenny, L. Krystyn, R. Wernli and L. Zaninetti. The authors are very obliged to Lausanne University, Switzerland for making available laboratory facilities, and especially to Laurent Nicod who prepared the thin sections. We are grateful to J. Metzger (University of Geneva) for help with computer drafting. P.M. is indebted to O. Parlak for offering the opportunity to visit the area around Mersin and to the Geological Department of the Süleyman Demirel University in Isparta (R. Karagüzel and Ö. Karaca) for field work logistics. He is also very grateful to Shell International Exploration and Production for financial support. Thoughtful reviews by O. Parlak and an anonymous reviewer significantly improved the final manuscript. A.M.C. Şengör is gratefully acknowledged for the Turkish translation of the title, abstract and key words.

References

ALTINER, D. 1981. *Recherches stratigraphiques et micropaléontologiques dans le Taurus Oriental au NW de Pınarbaşı (Turquie)*. PhD Thesis, Université de Genève, Switzerland.

AVŞAR, N. 1992. Namrun (İçel) yöresi paleojen bentik foraminifer faunası [Paleogene benthic foraminifera fauna of Namrun (İçel) region]. *Maden Tektik ve Arama Dergisi* **114**, 127–144 [in Turkish with English abstract].

BAGHERI, S., KOZUR, H.W. & STAMPFLI, G.M. 2003. The Paleotethys suture in NE Iran and its displaced continuation in Central Iran (Anarak-Nakhlak area). *22nd IAS Meeting, International Association of Sedimentology. Zbornik Radova Proceedings, Opatija, Croatia, Abstracts*, p. 9.

BAGHERI, S. & STAMPFLI, G.M. 2008. The Anarak, Jandaq and Posht-e-Badam metamorphic complexes in central Iran: new geological data, relationships and tectonic implications. *Tectonophysics* **451**, 123–155.

BAGHERI, S., STAMPFLI, G.M. & KOZUR, H.W. 2004. Tectonic evolution of displaced Palaeotethyan margins in Central Iran. *32nd International Geological Congress, Florence, Abstracts*, p. 729.

BAILEY, E.B. & MCCALLIEN, W.J. 1950. The Ankara mélange and the Anatolian thrust. *Nature* **166**, 938–940.

BAILEY, E.B. & MCCALLIEN, W.J. 1953. Serpentinites lavas, the Ankara melange and the Anatolian thrust. *Transaction of the Royal Society of Edinburgh* **62**, 403–442.

BLENDINGER, W., FURNISH, W.M. & GLENISTER, B.F. 1992. Permian cephalopod limestones, Oman Mountains: evidence for a Permian seaway along the northern margin of Gondwana. *Palaeogeography, Palaeoclimatology, Palaeoecology* **93**, 13–20.

BOZKURT, E. & MITTWEDE, S.K. 2001. Introduction of the geology of Turkey - a synthesis. *International Geology Review* **43**, 578–594.

BRINKMANN, R. 1976. *Geology of Turkey*. Elsevier Scientific Publishing Company, Amsterdam, Oxford, New York.

BRÖNNIMANN, P., POISSON, A. & ZANINETTI, L. 1970. L'unité de Domuz Dağ (Taurus lycien, Turquie). Microfaciès et foraminifères du Trias et du Lias. *Rivista Italiana di Paleontologia e Stratigrafia* **76**, 1–36.

CARCIONE L. 2007. *Sedimentology, Biostratigraphy and Mineralogy of the Lercara Formation (Triassic, Sicily) and Its Palaeogeographic Implications*. PhD Thesis, Université de Genève, Genève, Switzerland.

CATALANO, R., DI STEFANO, P. & KOZUR, H.W. 1991. Permian circumpacific deep-water faunas from the western Tethys (Sicily, Italy) – new evidence for the position of the Permian Tethys. *Palaeogeography, Palaeoclimatology, Palaeoecology* **87**, 75–108.

CATALANO, R., DI STEFANO, P. & KOZUR, H.W. 1992. New data on Permian and Triassic stratigraphy of western Sicily. *Neues Jahrbuch für Geologie und Paläontologie, Abhandlungen* **184**, 25–61.

Çelik, Ö.F. 2008. Detailed geochemistry and K-Ar geochronology of the metamorphic sole rocks and their mafic dykes from the Mersin ophiolite, southern Turkey. *Turkish Journal of Earth Sciences* **17**, 685–708.

Clark, M. & Robertson, A.H.F. 2002. The role of the Tertiary Ulukışla basin, southern Turkey, in suturing of the Mesozoic Tethys ocean. *Journal of the Geological Society, London* **159**, 673–690.

Crasquin-Soleau, S., Richoz, S., Marcoux, J., Angiolini, L., Nicora, A. & Baud, A. 2002. Les évènements de la limite Permien–Trias: derniers survivants et/ou premiers re-colonisateurs parmi les ostracodes du Taurus (Sud-Ouest de la Turquie) [The events of the Permian–Trias boundary: last survivors and/or first colonisers among the ostracods of the Taurides (southwestern Turkey)]. *Comptes Rendus Geosciences* **334**, 489–495.

Degnan, P.J. & Robertson, A.H.F. 1998. Mesozoic–Early Tertiary passive margin evolution of the Pindos Ocean (NW Peloponnese, Greece). *Sedimentary Geology* **117**, 33–70.

Delaune-Mayère, M., Marcoux, J., Parrot, J.-F. & Poisson, A. 1977. Modèle d'évolution mésozoique de la paléo-marge téthysienne au niveau des nappes radiolaritiques et ophiolitiques du Taurus Lycien d'Antalya et du Baër-Bassit. *In:* Biju-Duval, B. & Montadert, L. (eds), *Structural History of the Mediterranean Basins*. Editions Technip, Paris, 79–94.

Demirtaşli, E., Turhan, N., Bilgin, A.Z. & Selim, M. 1984. Geology of the Bolkar Mountains. *In:* Tekeli, O. & Göncüoğlu, M.C. (eds), *Geology of the Taurus Belt*. Maden Tektik ve Arama Enstitüsü, Ankara, Turkey, 125–141.

Dilek, Y., Thy, P., Hacker, B. & Grundvig, S. 1999. Structure and petrology of Tauride ophiolites and mafic intrusions (Turkey): implications for the Neotethyan Ocean. *Geological Society of America Bulletin* **111**, 1192–1216.

Dommergues, J.-L., Meister, C., Bonneau, M., Poisson, A. & Vrielinck, B. 2005. Les ammonites pliensbachiennes des nappes Lyciennes (Turquie méridionale). Description de faunes nouvelles, implications biostratigraphiques et paleobiogéographiques. *Geobios* **38**, 407–435.

Einor O.L. 1979. *Atlas Fauny i Flory Srednego-pozdnego Karbona Bashkirii*. Nedra, Moscow [in Russian].

Epstein, A.G., Epstein, J.B. & Harris, L.D. 1977. *Conodont Colour Alteration - An Index to Organic Metamorphism*. U.S. Geological Survey Professional Paper **995**, 1–27.

Gallet, Y., Krystyn, L., Marcoux, J. & Besse, J. 2007. New constraints on the end-Triassic (Upper Norian–Rhaetian) magnetostratigraphy. *Earth and Planetary Science Letters* **255**, 458–470.

Gansser, A. 1955. New aspects of the geology in Central Iran. Proceedings - *World Petroleum Congress* **59**, 279–300.

Gansser, A. 1974. The ophiolitic melange, a world-wide problem on Tethyan examples. *Eclogae Geologicae Helvetiae* **67**, 479–507.

Gerth, H. 1950. Die Ammonoideen des Perms von Timor und ihre Bedeutung für die stratigraphische Gliederung der Permformation. *Neues Jahrbuch für Mineralogie Geologie und Paläontologie, Abhandlungen* **91**, 233–320.

Gökdeniz, S. 1981. *Recherches géologiques dans les Taurides occidentales entre Karaman et Ermenek, Turquie. Les séries à 'tuffites vertes' triasiques*. PhD Thesis, Université de Paris Sud, centre d'Orsay, Paris, France.

Göncüoğlu, M.C., Kuwahara, K., Tekin, U.K. & Turhan, N. 2004. Upper Permian (Changxingian) radiolarian cherts within the clastic successions of the 'Karakaya complex' in NW Anatolia. *Turkish Journal of Earth Sciences* **13**, 201–213.

Göncüoğlu, C.M., Şenol, Ç., Gürsu, S., Noble, P., Turhan, N., Tekin, U.K., Okuyucu, C. & Göncüoğlu, Y. 2007. The Mississippian in the Central and Eastern Taurides (Turkey): constraints on the tectonic setting of the Tauride-Anatolide Platform. *Geologica Carpathica* **58**, 427–442.

Gradstein, F.M., Ogg, J.G., Smith, A.G., Agterberg, F.P., Bleeker, W., Cooper, R.A., Davydov, V., Gibbard, P., Hinnov, L., House, M.R., Lourens, L., Luterbacher, H.P., McArthur, J., Melchin, M.J., Robb, L.J., Shergold, J., Villeneuve, M., Wardlaw, B.R., Ali, J., Brinkhuis, H., Hilgen, F.J., Hooker, J., Howarth, R.J., Knoll, A.H., Laskar, J., Monechi, S., Plumb, K.A., Powell, J., Raffi, I., Roehl, U., Sanfilippo, A., Schmitz, B., Shackleton, N.J., Shields, G.A., Strauss, H., van Dam, J., van Kolfschoten, T., Veizer, J. & Wilson, D. 2004. *A Geological Time Scale 2004*. Miscellaneous Report - Geological Survey of Canada. Geological Survey of Canada. Ottawa, ON, Canada.

Greenly, E. 1919. *The Geology of Anglesey*. Great Britain Geological Survey Memoir **1**, 1–980.

Gutnic, M. & Monod, O. 1970. Une série mésozoïque condensée dans les nappes du Taurus occidental : la série du Boyalı Tepe. *Bulletin de la Société Géologique de France* **5**, 166–167.

Gutnic, M., Monod, O., Poisson, A. & Dumont, J.-F. 1979. Géologie des Taurides occidentales (Turquie). *Mémoire de la Société Géologique de France* **137**, Paris, 1–109.

Hsu, K.J. 1968. Principles of melanges and their bearing on the Franciscan-Knoxville paradox. *Geological Society of America Bulletin* **79**, 1063–1074.

Hungerbühler, A., Moix, P., Guex, J., Stampfli, G.M. & Marcoux, J. 2008. First evidence of Cordevolian (lower Carnian) radiolarians at the base of the Upper Antalya Nappes, Turkey, *33rd IGC, International Geological Congress, Abstract Volume on CD-ROM, Oslo, August 6–14th*, *Abstracts*.

Juteau, T. 1980. Ophiolites of Turkey. *Ofioliti* **2**, 199–238.

Kozitskaya, R.I., Kossenko, Z.A., Lipnyagov, O.M. & Nemirovskaya, T.I. 1978. *Konodontî karbona donetskogo basseyna*. Izd-vo Nauka Dumka, Kiev.

Kozur, H.W. 1990. Deep-Water Permian in Sicily and its possible connection with the Himalaya-Tibet region. *5th Himalaya-Tibet-Karakorum workshop. Dipartimento di Scienze della Terra, Università di Milano, Milano, Italy*, *Abstracts*.

KOZUR, H.W. 1993. Upper Permian Radiolarians from the Sosio Valley Area, Western Sicily (Italy) and from the Uppermost Lamar Limestone of West Texas. *Jahrbuch der Geologischen Bundesanstalt, Wien* **136**, 99–123.

KOZUR, H.W. 1995. First evidence of Middle Permian Ammonitico Rosso and further new stratigraphic results in the Permian and Triassic of the Sosio Valley area, Western Sicily. *1st Croatian Geological congress. Zbornik radova proceedings, Opatija*, *Abstracts*, 307–310.

KOZUR, H.W. 1997. Late Paleozoic and Early Mesozoic opening times of Tethyan oceanic and continental basins in Turkey. *Interrad VIII. Laboratoire de Géologie du Muséum de Paris, Paris*, *Abstracts*, p. 77.

KOZUR, H.W. 2003a. Integrated Permian ammonoid, conodont and radiolarian zonation of the Triassic. *Hallesches Jahrbuch für Geowissenschaften* **B 25**, 49–79.

KOZUR, H.W. 2003b. Integrated Permian ammonoid, conodont, fusulinid, marine ostracod and radiolarian biostratigraphy. *Permophiles* **42**, 24–33.

KOZUR, H.W., AYDIN, M., DEMİR, O., YAKAR, H., GÖNCÜOĞLU, M.C. & KURU, F. 2000. New stratigraphic and paleogeographic results from the Paleozoic and Early Mesozoic of the Middle Pontides (Northern Turkey) in the Azdavay, Devrekani, Küre and Inebolu areas: implications for the Carboniferous–Early Cretaceous geodynamic evolution and some related remarks to the Karakaya oceanic rift basin. *Geologia Croatica* **53**, 209–268.

KOZUR, H.W., MOIX, P. & OZSVÁRT, P. 2007a. Further new Nassellaria of the lower Tuvalian (Upper Triassic) Spongotortilispinus moixi Zone of the Huğlu Unit in the Mersin Mélange. *Bulletin de la Société vaudoise des Sciences Naturelles* **90**, 197–215.

KOZUR, H.W., MOIX, P. & OZSVÁRT, P. 2007b. Stratigraphically important Spumellaria and Entactinaria from the lower Tuvalian (Upper Triassic) of the Huğlu Unit in the Mersin Mélange, southeastern Turkey. *Bulletin de la Société vaudoise des Sciences Naturelles* **90**, 175–195.

KOZUR, H.W., MOIX, P. & OZSVÁRT, P. 2007c. Characteristic Nassellaria of the lower Tuvalian (Upper Triassic) Spongotortilispinus moixi Zone of the Huğlu Unit in the Mersin Mélange, southeastern Turkey. *Bulletin de la Société vaudoise des Sciences Naturelles* **90**, 151–173.

KOZUR, H.W., MOIX, P. & OZSVÁRT, P. 2009. New Spumellaria (Radiolaria) from the early Tuvalian *Spongotortilispinus moixi* zone of Southeastern Turkey, with some remarks on the age of this fauna. *Jahrbuch der Geologischen Bundesanstalt* **149**, 25–59.

KOZUR, H.W. & MOSTLER, H. 1991. Pelagic Permian conodonts from an oceanic sequence at Sang-e-Sefid (Fariman, NE-Iran). *In:* RUTTNER, A.W. (ed), *The Triassic of Aghdarband (Aq Darband), NE-Iran and Its Pre-Triassic Frame*. Abhandlungen der Geologischen Bundesanstalt, 101–110.

KOZUR, H.W., ŞENEL, M. & TEKİN, K. 1998. First evidence of Hercynian Lower Carboniferous deep-water sediments in the Lycian Nappes, SW Turkey. *Geologica Croatica* **51**, 15–22.

LAPIERRE, H. 1975. Les formations sédimentaires et éruptives des Nappes de Mamonia et leurs relations avec le massif du Troodos. *Mémoires de la Société Géologique de France* **123**, 1–132.

LYS, M. 1986. *Biostratigraphie du Carbonifere et du Permien en Mésogée (Espagne, Afrique du Nord, Régions Egéennes, Proche-Orient); études micropaléontologiques (Foraminiferes), paléobiogeographie*. PhD Thesis, Paris-Sud, Centre d'Orsay, Paris, France.

MARCOUX, J. 1987. *Histoire et topologie de la Neo-Tethys - Tome 1 (introduction générale)*. PhD Thesis, Université Pierre et Marie Curie - Paris VI, Paris, France.

MARCOUX, J., BAUD, A., KRYSTYN, L. & MONOD, O. 1986. Late Permian and Triassic in Western Turkey. *In:* MARCOUX, J. (ed), *Guide Book Part 2*. Field Workshop.

MARTINI, R., PEYBERNÈS, B. & MOIX, P. 2009. Late Triassic foraminifera in reefal limestones of SW Cyprus. *Journal of Foraminiferal Research* **39**, 218–230.

MASSET, O. & MOIX, P. 2004. *Les mélanges de l'ophiolite de Mersin (Turquie du Sud)*. MSc Thesis, Lausanne, Switzerland [unpublished].

MOIX, P. 2010. *Contribution to the Geology of Southern Turkey: New Insights from the Mersin Mélanges and from the Lycian and Antalya Nappes*. PhD Thesis, Université de Lausanne, Lausanne, Switzerland [un published].

MOIX, P., BECCALETTO, L., KOZUR, H.W., HOCHARD, C., ROSSELET, F. & STAMPFLI, G.M. 2008a. A new classification of the Turkish terranes and sutures and its implication for the paleotectonic history of the region. *Tectonophysics* **451**, 7–39.

MOIX, P., CHAMPOD, E. & STAMPFLI, G.M. 2008b. The Triassic detrital units in southern Turkey: synrift or syncollisional series? *6th Swiss Geosciences Meeting, Lugano, 21st–23rd November 2008*, *Abstracts*, p. 48–49.

MOIX, P., KOZUR, H.W. & STAMPFLI, G.M. 2007a. Evidence for Palaeotethyan origin of a part of the Mersin Mélange (southern Turkey). *EGU, Geophysical Research Abstract* **9**, 08739, Vienna.

MOIX, P., KOZUR, H.W., STAMPFLI, G.M. & MOSTLER, H. 2007b. New palaeontological, biostratigraphical and palaeogeographical results from the Triassic of the Mersin mélange, SE Turkey. *In:* LUCAS, S.G. & SPIELMANN, J.A. (eds), *The Global Triassic*. New Mexico Museum of Natural History and Science Bulletin **41**, Albuquerque, 282–311.

MOIX, P. & STAMPFLI, G.M. 2009. The Triassic detrital units in the East-Mediterranean realm: back-arcs opening and Cimmerian collision. *EGU. Geophysical Research Abstracts*, **11**, Vienna.

MOIX, P., VACHARD, D., MARTINI, R., STAMPFLI, G.M., PILLE, L. & WERNLI, R. 2007c. New Carboniferous, Permian and Triassic results from the Lycian Nappes (south-western Turkey): paleogeographic implications, *5th Swiss Geosciences Meeting, Geneva*, *Abstracts*, 207–209.

Monod O. 1977. *Recherches géologiques dans le Taurus occidental au Sud de Beyşehir (Turquie)*. PhD Thesis, Université de Paris-Sud, Orsay, France.

Niko, S., Pillevuit, A. & Nishida, T. 1996. Early Late Permian (Wordian) non-ammonoid cephalopods from the Hamrat Duru Group, central Oman Mountains. *Transactions and Proceedings of the Paleontological Society of Japan (New Series)* **183**, 522–527.

Noble, P.J., Tekin, U.K., Gedik, I. & Pehlivan, S. 2008. Middle to Upper Tournaisian radiolaria of the Baltalimanı Formation, İstanbul, Turkey. *Journal of Paleontology* **82**, 37–56.

Norman, T.N. 1993. Remobilization of two mélanges in Central Anatolia. *Geological Journal* **28**, 267–275.

Okay, A.I. & Altiner, D. 2007. A condensed Mesozoic succession North of İzmir: a fragment of the Anatolide-Tauride platform in the Bornova flysch zone. *Turkish Journal of Earth Sciences* **16**, 1–23.

Okay, A.I. & Mostler, H. 1994. Carboniferous and Permian radiolarite blocks from the Karakaya complex in Northwest Turkey. *Turkish Journal of Earth Sciences* **3**, 23–28.

Okay, A.I. & Tüysüz, O. 1999. Tethyan Sutures of northern Turkey. *In:* Durand, B., Jolivet, L., Horvath, F. & Seranne, M. (eds), *Mediterranean Basins: Tertiary Extension Within the Alpine Orogen*. Geological Society, London, Special Publications **156**, 475–515.

Özer, E., Koç, H. & Özsayar, T.Y. 2004. Stratigraphical evidence for the depression of the northern margin of the Menderes-Tauride Block (Turkey) during the Late Cretaceous. *Journal of Asian Earth Sciences* **22**, 401–412.

Özgül, N. 1976. Torosların bazı temel jeoloji özellikleri [Basic geologic characteristics of Taurides]. *Türkiye Jeoloji Kurumu Bülteni* **19**, 65–78 [in Turkish with English abstract].

Özgül, N. 1984. Stratigraphy and tectonic evolution of the central Taurides. *In:* Tekeli, O. & Göncüoğlu, M.C. (eds), *Geology of the Taurus Belt*. Maden Tetkik ve Arama Enstitüsü, Ankara, Turkey, 77–90.

Özgül, N. 1997. Bozkır-Hadim-Taşkent (orta Toroslar'ın kuzey kesimi) dolayında yer alan tektono-stratigrafik birliklerin stratigrafisi [Stratigraphy of tectono-stratigraphic units in Bozkır-Hadim-Taşkent (northern side of central Taurides) area]. *Maden Tektik ve Arama Dergisi* **119**, 113–174 [in Turkish with English abstract].

Pampal, S. 1984. Arslanköy-Tepeköy (Mersin) yöresinin jeolojisi [Geology of Arslanköy-Tepeköy (Mersin) region]. *Selçuk Universitesi - Fen-Edebiyat Fakültesi Fen Dergisi* **3**, 247–258 [in Turkish with English abstract].

Pampal, S. 1987. Güzeloluk-Sorgun (Mersin) yöresinin jeolojisi [Geology of Güzeloluk-Sorgun (Mersin) region]. *Gazi Üniversitesi-Mühendislik Mimarlık Dakültesi Dergisi* **1**, 143–174 [in Turkish with English abstract].

Pampal, S. & Kurtman, F. 1984. New data on the Neo-tethys rifting in the Eastern Taurus region. *In:* Tekeli, O. & Göncüoğlu, C.M. (eds), *Geology of the Taurus Belt*. Maden Tetkik ve Arama Enstitüsü, Ankara, Turkey, 217–222.

Parlak, O. 1996. *Geochemistry and Geochronology of the Mersin Ophiolite Within the Eastern Mediterranean Tectonic Frame (Southern Turkey)*. PhD Thesis, Université de Genève, Genève, Switzerland.

Parlak, O., Bozkurt, E. & Delaloye, M. 1996a. The obduction direction of the Mersin ophiolite: structural evidence from subophiolitic metamorphics in the Central Tauride Belt, Southern Turkey. *International Geology Review* **38**, 778–786.

Parlak, O. & Delaloye, M. 1996. Geochemistry and timing of postmetamorphic dike emplacement in the Mersin ophiolite (southern Turkey): new age constraints from ^{40}Ar-^{39}Ar geochronology. *Terra Nova* **8**, 585–592.

Parlak, O. & Delaloye, M. 1999. Precise ^{40}Ar-^{39}Ar ages from the metamorphic sole of the Mersin ophiolite (southern Turkey). *Tectonophysics* **301**, 145–158.

Parlak, O., Delaloye, M. & Bingöl, E., 1995. Origin of sub-ophiolitic metamorphic rocks beneath the Mersin ophiolite, Southern Turkey. *Ofioliti* **20**, 97–110.

Parlak, O., Delaloye, M. & Bingöl, E. 1996b. Mineral chemistry of ultramafic and mafic cumulates as an indicator of the arc-related origin of the Mersin ophiolite (Southern Turkey). *Geologischen Rundschau* **85**, 647–661.

Parlak, O. & Robertson, A.H.F. 2004. The ophiolite-related Mersin Mélange, southern Turkey; its role in the tectonic-sedimentary setting of Tethys in the Eastern Mediterranean region. *Geological Magazine* **141**, 257–286.

Poisson, A. 1977. *Recherches géologiques dans les Taurides occidentales (Turquie)*. PhD Thesis, Paris-Sud (centre d'Orsay), Paris, France.

Raymond, L.A. 1984. Classification of mélanges. *In:* Raymond, L.A. (ed), *Mélanges: Their Nature, Origin and Significance*. Geological Society of America, Boulder, Colorado, 7–20.

Raymond, L.A. & Terranova, T. 1984. Prologue – The melange problem – a review. *In:* Raymond, L.A. (ed), *Melanges: Their Nature, Origin and Significance*. Geological Society of America, Boulder, Colorado, 1–5.

Rejebian, V.A., Harris, A.G. & Hueber, J.S. 1987. Conodont color and textural alteration–an index to regional metamorphism and hydrothermal alteration. *Geological Society of America Bulletin* **99**, 471–479.

Ricou, L.-E., Argyriadis, I. & Marcoux, J. 1975. L'axe calcaire du Taurus, un alignement de fenêtres arabo-africaines sous des nappes radiolaritiques, ophiolitiques et métamorphiques. *Bulletin de la Société Géologique de France* **17**, 1024–1044.

Ricou, L.-E., Marcoux, J. & Whitechurch, H. 1984. The Mesozoic organization of the Taurides: one or several ocean basins? *In:* Dixon, J.E. & Robertson, A.H.F. (eds), *The Geological Evolution of the Eastern Mediterranean*. Geological Society, London, Special Publications **17**, 349–359.

ROBERTSON, A.H.F., PARLAK, O., RIZAOĞLU, T., ÜNLÜGENÇ, U., İNAN, N., TASLI, K. & USTAÖMER, T. 2007. Tectonic evolution of the south Tethyan Ocean; evidence from the eastern Taurus Mountains (Elazığ region, SE Turkey). *In*: RIES, A.C., BUTLER, R.W.H. & GRAHAM, R.H. (eds), *Deformation of the Continental Crust: The Legacy of Mike Coward*. Geological Society, London, Special Publications **272**, 231–270.

ROBERTSON, A.H.F., PARLAK, O. & USTAÖMER, T. 2009. Mélange genesis and ophiolite emplacement related to subduction of the northern margin of the Tauride-Anatolide continent, central and western Turkey. *In*: VAN HINSBERGEN, D.J.J., EDWARDS, M.A. & GOVERS, R. (eds), *Collision and Collapse at the Africa-Arabia-Eurasia Subduction Zone*. Geological Society, London, Special Publications **311**, 9–66.

ROBERTSON, A.H.F., USTAÖMER, T., PARLAK, O., ÜNLÜGENÇ, U.C., TAŞLI, K. & İNAN, N. 2006. The Berit transect of the Tauride thrust belt, S Turkey: Late Cretaceous–Early Cenozoic accretionary/collisional processes related to closure of the Southern Neotethys. *Journal of Asian Earth Sciences* **27**, 108–145.

ROGHI, G., MIETTO, P. & DALLA VECCHIA, F.M. 1995. Contribution to the conodont biostratigraphy of the Dolomia di Forni (Upper Triassic, Carnia, NE Italy). *Memorie di Scienze Geologiche, Padova*, 125–133.

ŞENGÖR, A.M.C. & YILMAZ, Y. 1981. Tethyan evolution of Turkey: a plate tectonic approach. *Tectonophysics*, **75**, 181–241.

SILVER, E.A. & BEUTNER, E.C. 1980. Melanges. *Geology* **8**, 32–34.

SONE, M., LEMAN, M.S. & EHIRO, M. 2001. Middle Permian cephalopods from central Peninsular Malaysia; implications for faunal migration through the southern Tethys. *Journal of Asian Earth Sciences* **19**, 805–814.

STAMPFLI, G.M. 2000. Tethyan oceans. *In:* BOZKURT, E., WINCHESTER, J.A. & PIPER, J.D.A. (eds), *Tectonics and Magmatism in Turkey and Surrounding Area*. Geological Society, London, Special Publications **173**, 1–23.

STAMPFLI, G.M. & KOZUR, H.W. 2006. Europe from the Variscan to the Alpine cycles. *In:* GEE, D.G. & STEPHENSON, R.A. (eds), *European Lithosphere Dynamics*. Memoir of the Geological Society, London, 57–82.

STAMPFLI, G.M., MOSAR, J., FAVRE, P., PILLEVUIT, A. & VANNAY, J.-C. 2001. Permo–Mesozoic evolution of the western Tethyan realm: the Neotethys/East-Mediterranean connection. *In:* ZIEGLER, P.A., CAVAZZA, W., ROBERTSON, A.H.F. & CRASQUIN-SOLEAU, S. (eds), *PeriTethys Memoir 6: Peritethyan Rift/Wrench Basins and Passive Margins*. IGCP 369 Mémoires du Museum National d'Histoire Naturelle, Paris, 51–108.

STAMPFLI, G.M., VAVASSIS, I., DE BONO, A., ROSSELET, F., MATTI, B. & BELLINI, M. 2003. Remnants of the Palaeotethys oceanic suture-zone in the western Tethyan area. *In:* CASSINIS, G. & DECANDIA, F.A. (eds), *Stratigraphic and Structural Evolution on the Late Carboniferous to Triassic Continental and Marine Successions in Tuscany (Italy): Regional Reports and General Correlation*. Bolletino della Società Geologica Italiana, Volume speciale, 1–24.

TAŞLI, K., ÖZER, E. & KOÇ, H. 2006. Benthic foraminiferal assemblages of the Cretaceous platform carbonate succession in the Yavca area (Bolkar Mountains, S Turkey): biostratigraphy and paleoenvironments. *Geobios* **39**, 521–533.

TEKİN, U.K. 1999. Biostratigraphy and systematics of late Middle to Late Triassic radiolarians from the Taurus Mountains and Ankara region, Turkey. *Geologisch-Paläontologische Mitteilungen Innsbruck, Sonderband* **5**, 1–296.

TEKİN, U.K. & BEDİ, Y. 2007a. Ruesticyrtiidae (Radiolaria) from the middle Carnian (Late Triassic) of Köseyahya Nappe (Elbistan, eastern Turkey). *Geologica Carpathica* **58**, 153–167.

TEKİN, U.K. & BEDİ, Y. 2007b. Middle Carnian (Late Triassic) Nassellaria (Radiolaria) of Köseyahya Nappe from eastern Taurides, eastern Turkey. *Rivista Italiana di Paleontologia e Stratigrafia* **113**, 167–190.

TEKİN, U.K., EKMEKÇİ, E. & KOZUR, H.W. 2001. Dating of the Huğlu tuffite based on the radiolarian fauna, Huğlu Unit (Beyşehir-Hoyran Nappes), Central Taurides, Turkey. *4th International Geology Symposium, Abstracts*, p. 264.

THUIZAT, R., WHITECHURCH, H., MONTIGNY, R. & JUTEAU, T. 1981. K-Ar dating of some infra-ophiolitic metamorphic soles from the Eastern Mediterranean: new evidence for oceanic thrustings before obduction. *Earth and Planetary Science Letters* **52**, 302–310.

TSOFLIAS, P. 1969. Sur la découverte d'Ammonites triasiques au front de la nappe du Pinde en Péloponnèse septentrional (Grèce). *Comptes Rendus Sommaires des Séances de la Société géologique de France* **4**, p. 118.

VACHARD, D. & MOIX, P. in review. Late Pennsylvanian to Middle Permian revised biostratigraphy and palaeobiogeography of the Lycian Nappes (SW Turkey). *Revue de Micropaléontologie.*

VAŠÍČEK, Z. & KULLMANN, J. 1988. Eine Ammonoideen-Fauna vom Sosio-Typ (Guadalupian, Ober-Perm) aus Kurdistan (Irak). *Paleontographica Abteilung A* **204**, 95–115.

WIGNALL, P.B., NEWTON, R. & BROOKFIELD, M.E. 2005. Pyrite framboid evidence for oxygen-poor deposition during the Permian-Triassic crisis in Kashmir. *Palaeogeography, Palaeoclimatology, Palaeoecology* **216**, 183–188.

WILKIN, R.T. & BARNES, H.L. 1997. Formation processes of framboidal pyrite. *Geochimica et Cosmochimica Acta* **61**, 323–339.

PLATE 1

Late Serpukhovian to Middle Permian bioclasts.

Figures 1–3. Late Serpukhovian. Sample 393.
Figure 1. Detail of a broad dendrolite of *Praedonezella* cf. *cespeformis* Kulik.
Figure 2. *Terebella* (worm burrow) within a microbialitic biopelmicrite (thrombolite).
Figure 3. *Plectostaffella* cf. *varvariensiformis* Brazhnikova & Vdovenko. Axial section. Late Serpukhovian. Sample 393.
Figures 4–8. Bashkirian. Sample MM144
Figure 4. *Asteroarchaediscus postrugosus* (Reitlinger). Axial section.
Figure 5. *Cornuspira multivoluta* (Reitlinger). Axial section.
Figure 6. *Anthracoporellopsis machaevii* Maslov; subaxial section **(a)** and two oblique sections of *Cornuspira multivoluta* **(b–c)**.
Figure 7. *Ozawainella* aff. *digitalis* Manukalova. Subaxial section with an attached *Hemithurammina fimbriata* (Howchin) emend. Mamet (right, bottom).
Figure 8. *Iricinella spirilliniformis* (Brazhnikova & Potievskaya). Subtransverse section.
Figures 9–18. Bioclasts of different ages reworked in a post-Asselian microbrecciated rudstone. Sample MM092.
Figure 9. *Fusulinella* sp. Subtransverse section. Reworked late Moscovian.
Figure 10. *Obsoletes* sp. Subaxial section. Reworked early Kasimovian.
Figure 11. *Asteroarchaediscus baschkiricus* (Krestovnikov & Teodorovich). Axial section. Reworked Serpukhovian or Bashkirian.
Figure 12. *Iriclinella* sp. Transverse section **(a)** with *Ungdarella* sp. (axial section). Reworked Bashkirian.
Figure 13. *Pseudostaffella* ex gr. *antiqua* (Dutkevich) (associated with big oolites, which can be used as secondary markers). Reworked early Bashkirian.
Figure 14. *Bradyina lucida* Morozova emend. Pinard & Mamet. Reworked Pennsylvanian.
Figure 15. *Rauserites* sp. Axial section. Reworked Gzhelian.
Figure 16. *Beresella* sp. Axial sections. Reworked Moscovian.
Figure 17. *Archaeolithoporella hidensis* Endô. Reworked Capitanian.
Figure 18. *Tubiphytes obscurus* Maslov, with an attached *Archaeolithoporella hidensis* Endô. Reworked Capitanian.

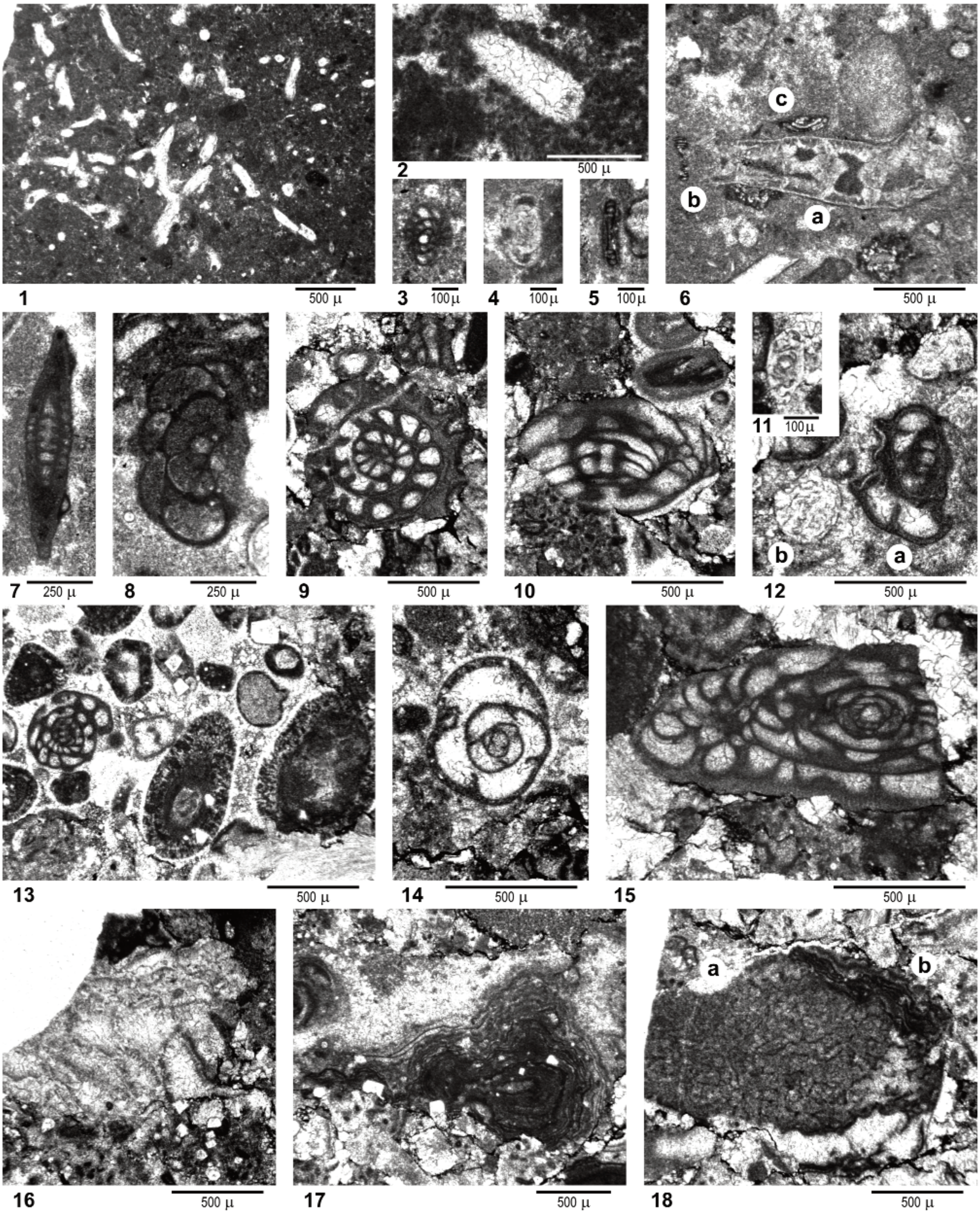
1
500 µ
2
500 µ
3
100µ
4
100µ
5
100µ
6
500 µ
a
b
c
7
250 µ
8
250 µ
9
500 µ
10
500 µ
11
100µ
12
500 µ
a
b
13
500 µ
14
500 µ
15
500 µ
16
500 µ
17
500 µ
18
500 µ
a
b

PLATE 2

Triassic and Cretaceous radiolarians from the Late Cretaceous Sorgun ophiolitic mélange. On each illustration, the SEM number is indicated. Rock samples, residues and illustrated specimens are stored in the collection of the first author. All scale bars = 100 microns.

Figure A. *Pseudostylosphaera* sp., 353-R18-02.

Figure B. *Muelleritortis*? sp., 353-R18-03.

Figure C. *Xitus* cf. *mclaughlini* Pessagno, MM019-R07-01.

Figures D, N. *Pseudodictyomitra* aff. *pseudomacrocephala* (Squinabol), D– MM019-R07-02, N– MM019-R07-12.

Figures E, G, J. *Dictyomitra* sp. E– MM019-R07-03, G– MM019-R07-05, J– MM019-R07-08.

Figure F. *Archaeodictyomitra* sp., MM019-R07-04.

Figures H, K, L, M, O, P. *Dictyomitra kozlovae* Foreman gr.: H– MM019-R07-06, K– MM019-R07-09, L– MM019-R07-10, M– MM019-R07-11, O– MM019-R07-13, P– MM019-R07-14.

Figure Q. *Dictyomitra* cf. *formosa* Squinabol MM019-R07-15.

Figure I. *Holocryptocapsa cryptodon* Dumitrică, MM019-R07-07.

Figure R. *Praexitus alievi* (Foreman), 316-R16-01.

Figure S. *Suna hybum* (Foreman), 316-R16-02.

Figure T. *Xitus vermiculatus* (Renz), 316-R16-03.

Figures U, Y, AA, AB. *Dictyomitra communis* (Squinabol), U– 316-R16-05, Y– 316-R16-10, AA– 316-R16-12, AB– 316-R16-13.

Figure V. *Hiscocapsa asseni* (Tan), 316-R16-06.

Figure W. *Pseudoeucyrtis zhamoidai* (Foreman), 316-R16-07.

Figure X. *Pseudodictyomitra carpatica* (Lozinyak), 316-R16-09.

Figure Z. *Pseudodictyomitra lilyae* (Tan), 316-R16-11.

Figure AC. *Pseudodictyomitra* cf. *thurowi* Dumitrică, 316-R16-14.

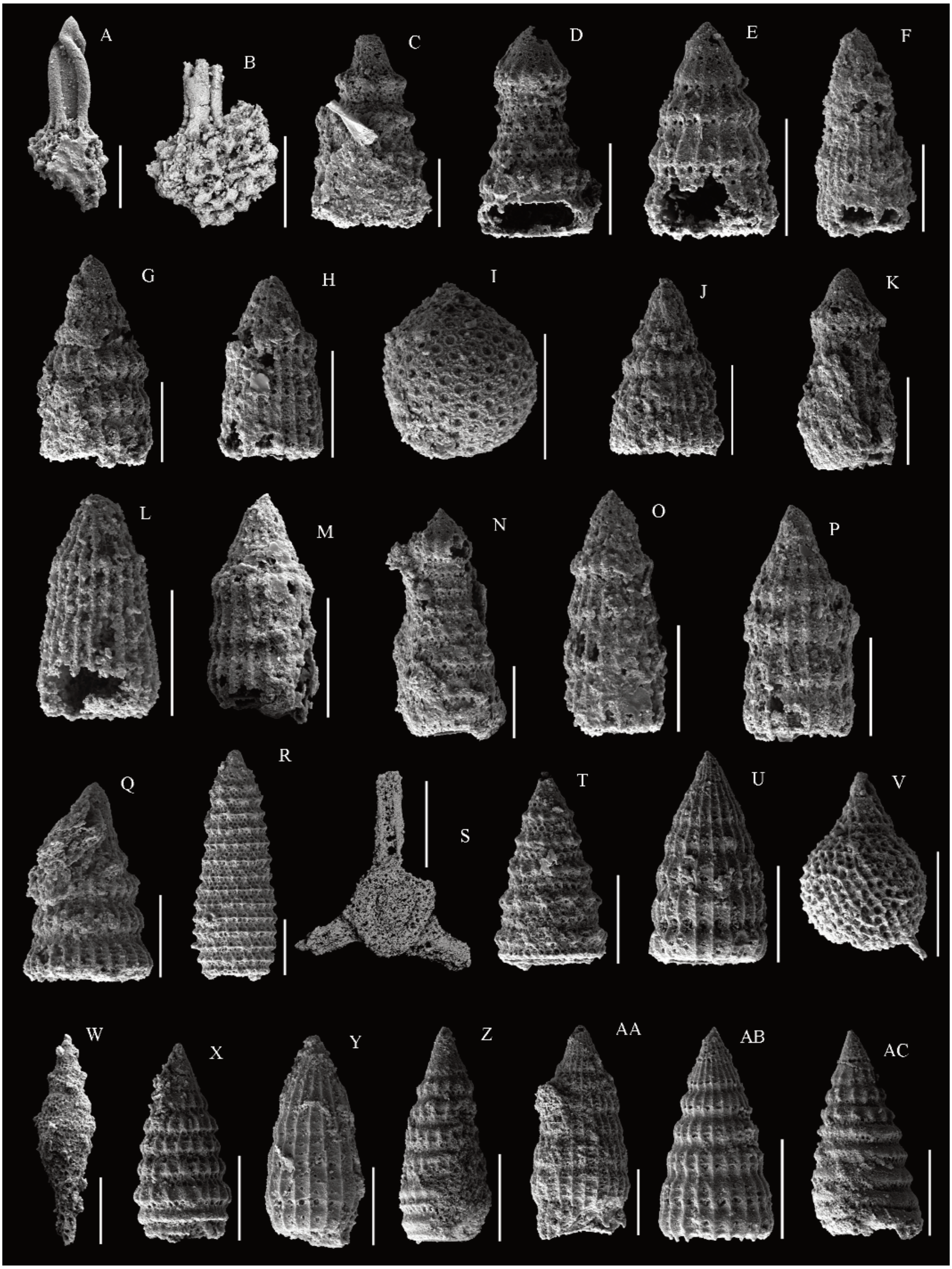
A
B
C
D
E
F
G
H
I
J
K
L
M
N
O
P
Q
R
S
T
U
V
W
X
Y
Z
AA
AB
AC

PLATE 3

Permian, Triassic and Jurassic radiolaria from the Late Cretaceous Sorgun ophiolitic mélange and from the Ladinian-Carnian Hacialanı mélange. On each illustration, the SEM number is indicated. Rock samples, residues and illustrated specimens are stored in the collection of the first author. All scale bars = 100 microns.

Figure A. *Annulotriassocampe* sp., G19-R10-01.
Figure B, ?*Livarella densiporata* Kozur & Mostler, G19-R10-02.
Figures C, I. *Archaeospongoprunum imlayi* Pessagno, C– 339-R11-02, I– 339-R11-11.
Figure D. *Transhsuum medium* Takemura, 339-R11-03.
Figure E. *Transhsuum maxwelli* (Pessagno), 339-R11-05.
Figure F. *Paronaella broennimanni* Pessagno, 339-R11-06.
Figure G. *Napora* sp., 339-R11-09.
Figure H. *Protunuma costata* (Heitzer), 339-R11-10.
Figures J, K, L. *Pseudoalbaillella postscalprata* Ishiga. J– MM173-R03-01, K– MM173-R03-03, L– MM173-R03-04.
Figure M, N. *Quinqueremis* sp., M– MM173-R03-05, N– MM173-R03-06.
Figure O. ?*Pseudoalbaillella rhombothoracata* Ishiga & Imoto, MM173-R03-08.
Figure P. *Latentifistula* sp., MM173-R03-09.
Figure Q. *Gustefana*? sp., MM173-R03-10.
Figure R. *Ishigaum trifustis* De Wever & Caridroit, MM173-R03-11.
Figures S, U, W. *Spinodeflandrella*? sp., S– MM173-R03-12, U– MM173-R03-14, W– MM173-R03-16.
Figures T, V. *Spinodeflandrella* cf. *siciliensis* Kozur, T– MM173-R03-13, V– MM173-R03-15.
Figure X. *Spinodeflandrella* spec. indet., MM173-R03-17.
Figure Y. *Latentifistula* sp., MM173-R03-18.
Figure Z. Follicucullidae, gen. et sp. indet., MM173-R03-19.
Figures AA, AC. *Pseudoalbaillella eurasiatica* Kozur, Krainer & Mostler, AA– MM174-R04-01, AC– MM174-R04-04.
Figures AB, AE. *Parafollicucullus fusiformis* Holdsworth & Jones, AB– MM174-R04-02, AE– MM174-R04-03.
Figure AD. *Cauletella* cf. *manica* (De Wever & Caridroit), MM174-R04-05.

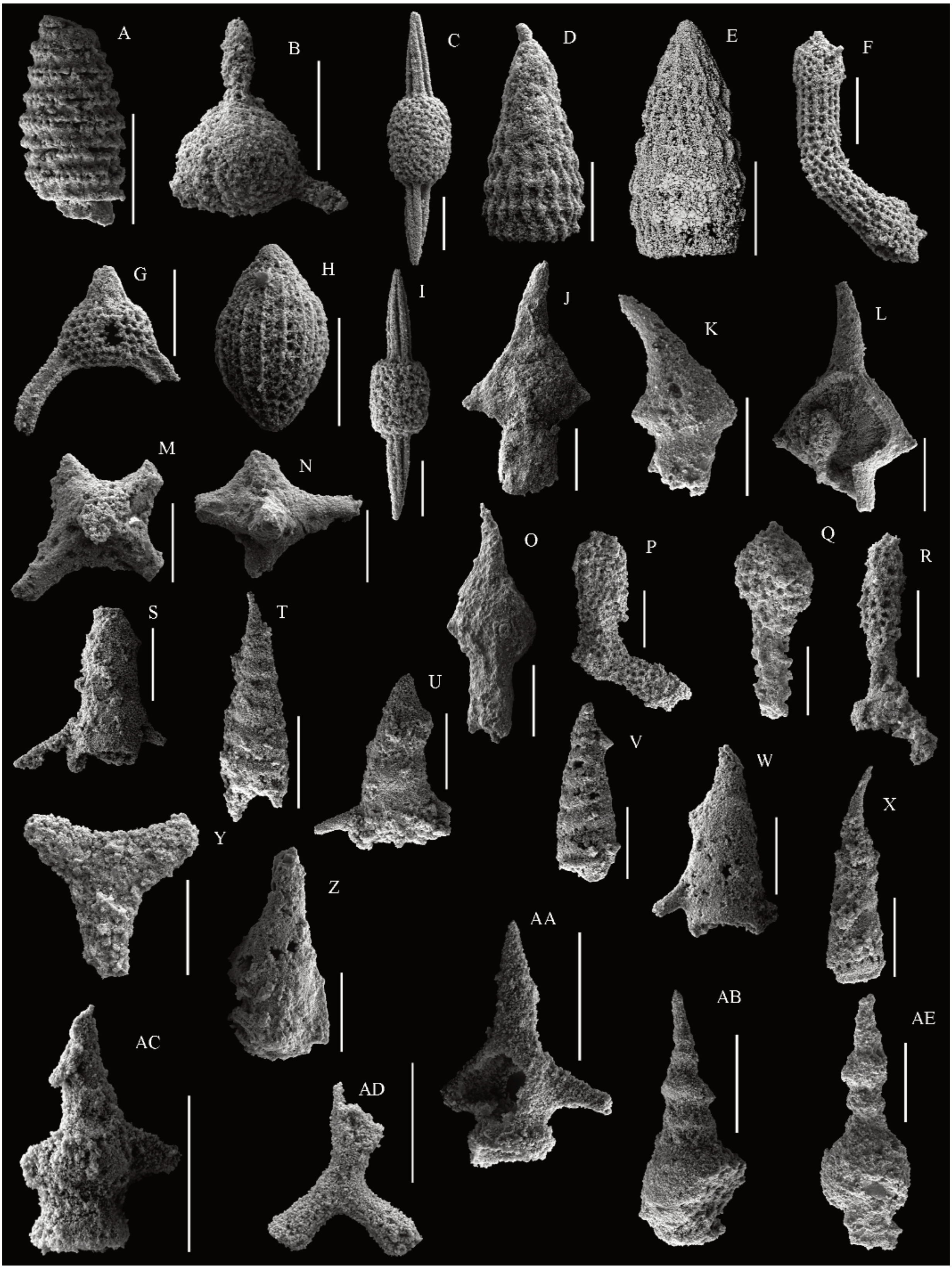
A
B
C
D
E
F
G
H
I
J
K
L
M
N
O
P
Q
R
S
T
U
V
W
X
Y
Z
AA
AB
AC
AD
AE

PLATE 4

Figures 1–7. Early Asselian breccia. Sample M2.
Figure 1. *Asselodiscus davydovi* Vachard and Moix, in review (nomen nudum). Axial section.
Figure 2. *Pseudovidalina modificata* (Potievskaya). Axial section.
Figure 3. *Boultonia* sp. (a) (subaxial section) and *Schubertella* sp. (b) (subtransverse section).
Figure 4. *Spireitlina*? sp. Transverse section.
Figure 5. *Globivalvulina vulgaris* Morozova. Oblique section.
Figure 6. *Schubertella* ex gr. *paramelonica* Suleimanov **(a)** (axial section) and *Tuberitina* sp. **(b)**.
Figure 7. *Kamaena* sp. Axial section.
Figures 8–9. Capitanian reworked bioclasts and microfacies of sample 378.
Figure 8. *Reichelina* sp. Subtransverse section.
Figure 9. Microfacies of microrudstone with fragments of volcanites (a, b).
Figures 10, 11. Bioclasts of sample 325.
Figure 10. *Dunbarula schubertellaeformis* Sheng. Axial section.
Figure 11. *Calvezina ottomana* Sellier de Civrieux & Dessauvagie. Axial section.
Figures 12–17. Reworked material of sample 355.
Figure 12. *Dvinella comata* Khvorova. Two axial sections (a, b).
Figure 13. *Schubertella kingi exilis* Suleimanov. Axial section.
Figure 14. *Schubertella* ex gr. *melonica* Dunbar & Skinner. Axial section.
Figure 15. *Tubiphytes obscurus* Maslov (a) and *Archaeolithoporella hidensis* Endô (b).
Figure 16. Schwagerinoidea indet (a), *Schubertella* sp. (b), and *Ungdarella uralica* Maslov (c).
Figure 17. *Dvinella* sp. (a) and *Tubiphytes obscurus* Maslov (b).

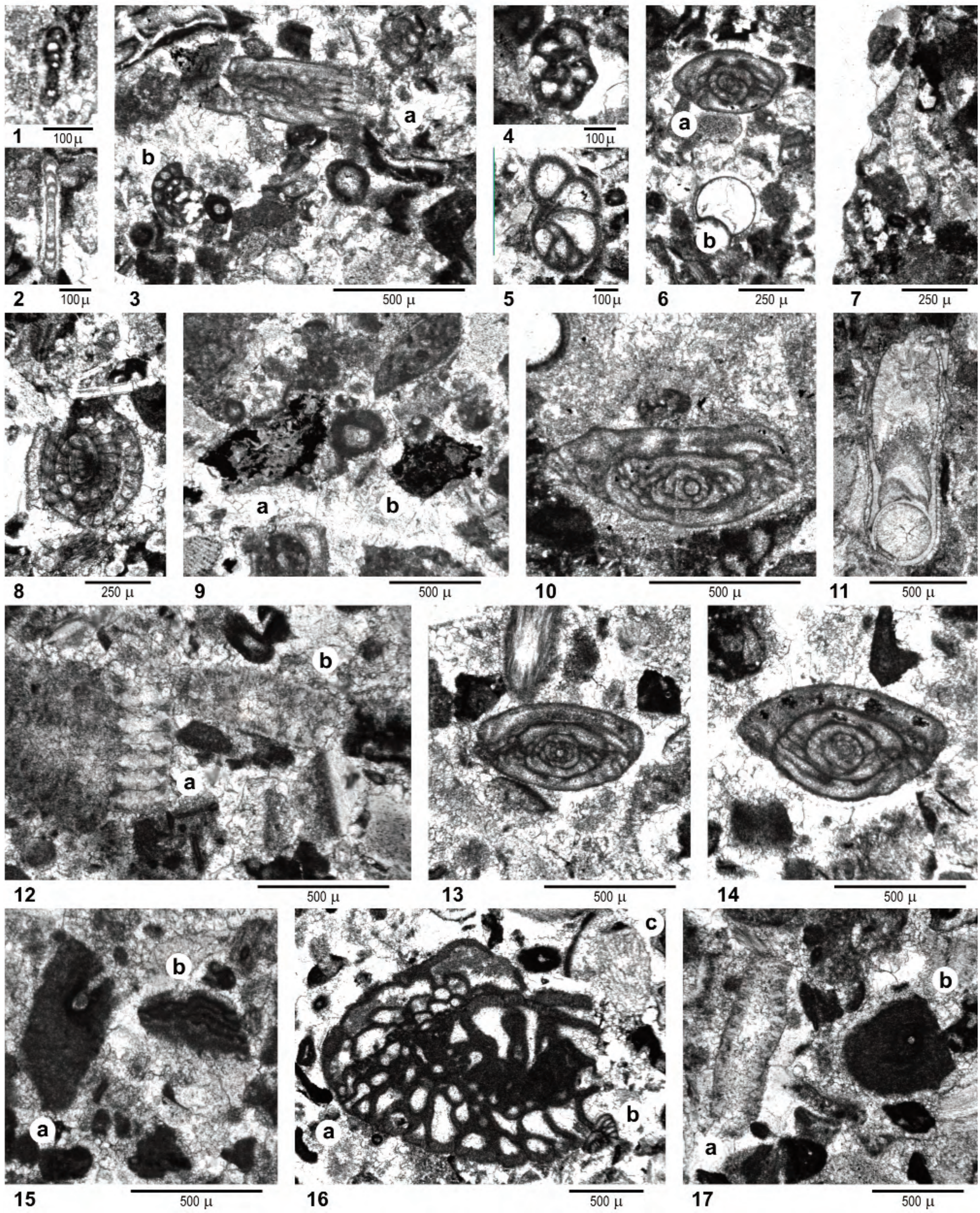
1
100 µ
2
100 µ
3
a
b
500 µ
4
100 µ
5
100 µ
6
a
b
250 µ
7
250 µ
8
250 µ
9
a
b
500 µ
10
500 µ
11
500 µ
12
a
b
500 µ
13
500 µ
14
500 µ
15
a
b
500 µ
16
a
b
c
500 µ
17
a
b
500 µ